Expansion of the HSV-2-specific T cell repertoire in skin after immunotherapeutic HSV-2 vaccine

Authors: Emily S. Ford[1,2], Alvason Li[1], Christine Johnston[1,2], Lichun Dong[2], Kurt Diem[3], Lichen Jing[2], Kerry J. Laing[2], Alexis Klock[3], Krithi Basu[2], Mariliis Ott[2], Jim Tartaglia[4], Sanjay Gurunathan[4], Jack L. Reid[5], Matyas Ecsedi[5], Aude G. Chapuis[5], Meei-Li Huang[3], Amalia S. Magaret[1,3], Jia Zhu[1,3], David M. Koelle[1,2,3,6,7], and Lawrence Corey[1,2,3]

Affiliations:
1Vaccine and Infectious Diseases Division, Fred Hutch Cancer Research Center, Seattle WA
2Division of Allergy and Infectious Diseases, Department of Medicine, University of Washington, Seattle WA
3Department of Laboratory Medicine and Pathology, University of Washington, Seattle WA
4Sanofi Pasteur, Swiftwater PA
5Clinical Research Division, Fred Hutch Cancer Research Center, Seattle WA
6Department of Global Health, University of Washington, Seattle WA
7Benaroya Research Institute, Seattle WA

ClinicalTrials.gov Identifier: NCT02571166

ABSTRACT

The skin at the site of HSV-2 reactivation is enriched for HSV-2 specific T cells. To evaluate whether an immunotherapeutic vaccine could elicit skin-based memory T cells we studied skin biopsies and HSV-2-reactive CD4+ T cells from peripheral blood mononuclear cells (PBMCs) by T-cell receptor (TCR) sequencing before and after vaccination with a replication-incompetent whole virus HSV-2 vaccine candidate (HSV529). The representation of HSV-2-reactive CD4+ T cell sequences from PBMCs increased from a median of 0.03% (range 0-0.09%) to 0.6% (range 0-1.3%) of the total skin TCR repertoire after the first vaccine dose. We found sustained expansion after vaccination in unique, skin-based T-cell clonotypes that were not detected in HSV-2-reactive CD4+ T cells isolated from PBMCs. While detection of skin clonotypes in the blood was related to abundance in the skin it was not related to expansion after vaccination. In one participant a switch in immunodominance was observed after vaccination with the emergence of a newly dominant TCRa/b pair in skin that was not detected in blood. We confirmed that the newly dominant clonotype was derived from an HSV-specific CD4+ T cell by creation of a synthetic TCR in a Jurkat-based cell line with a NR4A1-mNeonGreen reporter system. Our data indicate that the skin in areas of HSV-2 reactivation possesses an oligoclonal TCR repertoire that is distinct from the circulation with prominent clonotypes infrequently detected in the circulation by standard methods. Defining the influence of therapeutic vaccination on the HSV-2-specific TCR repertoire requires tissue-based evaluation.

INTRODUCTION

While antivirals for HSV-2 have been in widespread use for over 35 years, HSV-2 infection continues to be highly prevalent globally (1–3). As such, development of novel methods to curtail HSV-2 reactivation and transmission are needed. T cell immune responses are associated with severity and reactivation frequency of mucosal HSV infections (4,5), contributing to interest in the development of immunotherapeutic approaches to control HSV-2 reactivation. Although recombinant HSV-2 protein-based vaccines have been tested, and one demonstrated a partial but significant reduction in the rate of subclinical HSV-2 reactivation among seropositive adults (5–8), correlation between humoral or cellular markers of HSV-2 immunogenicity and vaccine response has not been demonstrated (5,8–11). Likewise, T cell responses in peripheral blood mononuclear cells (PBMCs) were not associated with efficacy in studies of peptide-based vaccines (12,13). Recently, in a Phase 1 study of HSV529, a replication-deficient HSV-2 whole virus vaccine, 46% of HSV-2-seropositive participants had a detectable increase in IFNγ expression in CD4+ T cells from PBMCs by ELISPOT (14). There was minimal (<10%) change in IFNγ expression from CD8+ T cells over the course of the vaccine trial.

Except during acute infection, HSV-specific CD4+ T cells comprise only a small percentage of circulating CD4+ T cells (15). T cell production of IFNγ or other cytokines in response to whole virus or peptide-based libraries is typically used to determine HSV specificity or activity (16–19). In a study of 40 HSV-2-seropositive individuals during clinical quiescence, 0.04-3.77% (median 0.31%) of CD4+ T cells from PBMCs expressed IFNγ after HSV-2 stimulation in vitro (20). As a surrogate marker of activation, HSV-specific CD4 and CD8 T cells can express CD137 after in

vitro exposure to antigen and antigen-presenting cells in activation-induced marker (AIM) assays (21). At present, cytokine production after cognate antigen exposure remains the gold standard to identify T cells with HSV specificity used in studies of vaccine response.

Data from animal models, corroborated by mathematical modeling of human data and observational human studies, have supported the importance of skin-resident memory T cells (TRM) in the adaptive immune responses to HSV-2 reactivation (22–27). These cells are distinct from skin-migratory T cells by phenotype, skin ingress and egress markers and spatial localization (27–29). A potential explanation for the lack of association between clinical benefit and measured immune response in immunotherapeutic vaccine trials is that the immune correlates of efficacy may lie in alteration of the immune responses in the genital or mucosal skin, rather than the response detected in circulating PBMCs.

To investigate whether a 3-dose vaccination series with HSV529 could elicit changes in the skin-based T-cell response, we performed T-cell receptor beta chain (TRB) repertoire sequencing of genital skin biopsies taken during clinical quiescence from the site of previous symptomatic HSV-2 reactivation before and after each dose. The TRB repertoire of HSV-2-enriched CD4+ T cells from PBMCs was sequenced to allow assignment of HSV-2-specificity among skin-identified clonotypes. CD4+ T cells were selected for comparison due to their observed expansion in the preceding phase 1 clinical trial (clinicaltrials.gov, NCT02571166). We found that an immunotherapeutic vaccination does elicit skin-based immune responses including expansion of HSV-2-specific T-cell clonotypes. Expansion in HSV-2-specific CD4 TRB clonotypes

targeting many, varied HSV-2 epitopes, were observed in blood. We also found sustained expansion after vaccination in unique, skin-based T-cell clonotypes that were not detected in HSV-2-reactive CD4+ T cells isolated from PBMCs. Tissue at the site of HSV-2 reactivation presents a unique compartment in which to study T cell responses to therapeutic vaccination. Technologies to measure the number, function and antigenic targets of skin-based immune responses are needed to enhance progress in the development of immunotherapeutic vaccines for recurrent HSV-2.

Materials and Methods:

Study design: This study was designed as an open-label Phase 1 study to observe the shifts in the TCR repertoire in the skin at the site of HSV-2 reactivation in comparison to HSV-2-reactive CD4+ T cells obtained from peripheral blood and biopsies from an uninvolved arm site over the course of a 6-month, 3-dose vaccination study with replication-incompetent vaccine candidate HSV529 (Sanofi). This study was specifically designed to evaluate whether immunologic changes occurred in sequential genital skin biopsies following HSV529 vaccination. Arm biopsies, lesion-site biopsies during a symptomatic lesion, and lesion-site biopsies following HSV suppression with acyclovir were used in each participant as internal controls – all participants received active vaccine (**Supplementary Table 1)**. Demographic information on the study participants is provided in **Supplementary Table 2**.

Participant recruitment and enrollment: Healthy men and women with a history of symptomatic genital herpes in areas amenable to biopsy were recruited to the University of Washington Virology Research Clinic (UW-VRC) in Seattle, WA. HSV-2 infection was confirmed by Western blot (40). Persons living with HIV were excluded. Participants provided informed consent to participate in the trial. The University of Washington Human Subjects Division approved the study procedures. The trial was monitored by a Data Safety Monitoring Board. The trial was registered on clinicaltrials.gov, NCT02571166.

Vaccine: The vaccine contained 0.5ml (1x 107pfu/dose) of HSV529, a replication-deficient, double-deletion (*UL5* and *UL29*) HSV-2 strain (Sanofi Pasteur)(41). Doses were delivered by intramuscular injection into the deltoid at days 0, 30 and 180. (**Supplementary Table 1**).

Genital-region skin biopsies: Genital site biopsies (3mm) were obtained at the site of HSV-2 reactivation, either confirmed by observation of a lesion at a study visit or by reported history. At enrollment, participants had a baseline genital biopsy performed at the site of a lesion, if present, or at the site of the most frequent recurrence, and received four weeks of valacyclovir 500mg daily to suppress HSV-2 reactivation. Participants stopped valacyclovir 3 days prior to vaccination. Genital skin biopsies were performed prior to each vaccine dose on days 0, 30, and 180, and 10 days after each dose at days 10, 40, and 190 (42). Non-genital skin biopsies were obtained from the arm at days 0, 10, 40 and 190. Biopsy samples were fresh frozen in optimum cutting temperature (OCT) compound.

DNA extraction and sequencing: A 1x3mm cross-section (inclusive of epidermis and dermis) from each biopsy was digested with proteinase-K and genomic DNA (gDNA) was extracted by spin column (Qiagen DNeasy). TCR sequencing was performed from gDNA samples by Adaptive Biotechnologies using the ImmunoSEQ assay (TCRβ chain)(33). TCRα chain sequencing (Adaptive Biotechnologies) from the same gDNA samples was performed for two participants. Adaptive TCR sequencing is a gDNA PCR-based platform in which the number of copies of each unique *CDR3* sequence (or TCR "clonotype") is directly proportional to the number of T cells bearing that sequence in each sample (34). In our experience, HSV-2-specific T-cell clonotypes with the same TCRβ *CDR3* nucleotide sequence may infrequently be paired with different TCRα sequences (43). The number of TCRβ sequence reads, or copy number, is therefore a surrogate for the number of clonotype-specific cells. *CDR3* nucleotide sequences were used to compare persistence and detection of a specific TCR clonotype within samples from a single participant. CDR3 amino acid sequences were used to compare TCR clonotype presence between participants.

Isolation of PBMCs: In the initial trial of HSV529, the majority of alterations in HSV-2 specific T-cell responses in PBMCs from HSV seronegative and HSV-2 seropositive participants were in the CD4+ T-cell population (42). HSV-2-reactive CD4+ T cells were enriched from PBMCs obtained at days 0 and 10 by two methods. In the first, PBMCs were incubated with UV-inactivated cell-associated HSV-2 (strain 186) for 18 hours, followed by sorting for live CD3+CD4+CD8-CD137high cells (modified from Jing *et al.*(21)). In the second, PBMCs were incubated with UV-inactivated HSV-2 for 18 hours, then selected for CD3+CD4+CD8- and accumulation of IFN-γ

and/or IL-2 by intracellular staining (modified from Moss *et al.*(20)). DNA was prepared with the Qiagen blood kit and TCR sequencing performed as above. In one participant (participant 4) the two selection procedures were performed iteratively to enhance the detection of HSV-2-reactive T cells from PBMCs. CD137+ cells were expanded polyclonally, tested for reactivity to UV-inactivated HSV-2 (HSV186), and stained for IFN-γ and IL-2 production (**Supplementary Fig. 1**). TCR sequencing of bulk cytokine-producing cells was performed as above.

Confirmation of HSV-2 specificity and determination of target epitope in PBMC-based clonotypes: Frozen PBMC from participant 4, day 10 after initial vaccination were incubated with UV-inactivated HSV-2 for 18 hours after which live CD3+CD4+CD137+ cells (n= 960) were single-cell sorted and cloned as published (17). We selected 192 random clones for functional screening with autologous irradiated PBMC as antigen-presenting cells (APC), UV-HSV-2 or UV-mock virus control as antigens, and tritiated thymidine incorporation proliferation assay as readout. We performed paired *TRA* and *TRB CDR3* sequencing on aliquots of ~ 100 cells per clone using a SMARTSeq-2 cDNA procedure (44). We then compared the *TRB CDR3* nucleotide sequences to those from biopsy skin from the same participant. The specificity of selected clones was determined to the level of the antigenic HSV-2 open reading frame (ORF) as previously described (38). Briefly, each HSV-2 ORF was cloned and expressed in vitro. T-cell clones were expanded once as described (18). HSV-2 proteins were arrayed as a matrix and queried as pools of 8 to 12 proteins/pool at final concentrations of ~1:5000 of each protein in proliferation assays. To confirm specificity, individual HSV-2 protein(s) at the intersection(s) of positive row and column pools were used as antigens in follow-up proliferation assays.

Development of reporter cell line: To create the NR4A1_NeonGreen TCR reporter, the coding sequence of mNeonGreen was integrated in-frame into the NR4A1 locus before the stop codon using CRISPR-induced homology directed repair (45). The mNeonGreen coding sequence (46) (IDT, Coralville IA) flanked by a 5' 334bp homology arm, 5' T2A element and a 315bp 3' homology arm was electroporated with recombinant spCas9 (IDT) and NR4A1 CRISPR guide RNA (IDT, sequence: AUGAAGAUCUUGUCAAUGAU) into Jurkat clone E6-1 cells (ATCC). Cells were cloned by limiting dilution and the clone with the highest signal upon PMA (5ng/ml) - ionomycin (5µg/ml) (Invivogen) stimulation was identified. The obtained reporter cell line was further modified by CRISPR KO of TCRa/b expression (gRNA sequences: AGAGUCUCUCAGCUGGUACA, CAAACACAGCGACCUUGGGU (IDT)); cells with successful KO were sorted for lack of CD3 expression. The final NR4A1_NeonGreen TCR reporter showed upregulation of the reporter signal according to TCR signal strength (Ecsedi et al. manuscript in preparation), mimicking regulation of the endogenous *NR4A1* locus (47).

Creation and HSV-2-specificity testing of synthetic TCR: Full-length, codon-optimized, TCR genes were synthesized (IDT) with TRB preceding a P2A sequence. TCR αβ pairing was promoted by partially replacing portions of the TRA and TRB constant regions with murine homologs with added cysteine residues. An epitope on the extracellular domain of murine TCRβ enabled flow cytometry monitoring of transduction as previously reported (48). The TCR inserts were cloned into pRRLSIN.cPPT.MSCV/GFP.WPRE (49) via Gibson assembly (New England Biolabs, Ipswich MA). After confirmation by sequencing, lentivirus was produced using a third-generation

system (Addgene, Watertown MA) on LentiX-293T cells (Takada Bio, Mountain View CA)(48). *Specificity Assay:* 200,000 synthetic TCR-transduced reporter cells were co-cultured with 200,000 participant-matched PBMC and 1/100 dilution of UV-irradiated HSV2186 virus or mock for 16-20 hours. Untransduced and PMA/Ionomycin-activated reporter cells were used as controls. Cells were labeled with Live Dead Aqua (Invitrogen) and anti-mouse TCR APC (BD Pharmingen) and analyzed on a FACS Canto II for expression of mNeongreen. *Protein-level Specificity Assay*: Protein-level specificity was assigned by measuring mNeongreen expression after 18-hour incubation of TCR-transduced reporter cells with matrix-pooled protein antigens spanning the HSV-2 proteome. Protein-level specificity was confirmed by a comparison between the HSV-2 protein of interest and a non-reacting protein at a range of concentrations (1:400 – 1:1600) for 18-24 hours. *Peptide-level Specificity Assay:* Peptide-level specificity was assigned by exposing the TCR-transduced reporter cells to pooled, linear peptides (1µg/ml) covering the UL49 sequence. *Blocking Assay:* Monoclonal antibodies to HLA-DP, DQ, and DR at a 1:40 final dilution were added to the specificity assays above in which UV-inactivated virus was also serially diluted (1:100, 1:1000) to determine HLA specificity (17).

Immunofluorescence staining: To evaluate the effects of vaccination on T-cell infiltration, we evaluated T-cell spatial localization and skin density as previously described (31). Thawed, 8µm skin sections were washed and fixed in acetone, stained for one hour in a casein solution (Vector Laboratories) at room temperature with mouse anti-human CD4 (1:1000; Biolegend), and tagged with Alexa-Fluor 488 by TSA amplification (Invitrogen), followed by staining with Alexa-Fluor 647-labeled mouse anti–human CD8+ (1:100; Caltag Laboratories) overnight at 4°C.

After nuclear staining with DAPI (Fluka), skin sections were mounted in Mowiol 40-88 containing 2.5% wt/vol DABCO (Sigma-Aldrich). Images were captured with Nikon Eclipse Ti with NIS-Elements Software and viewed in Fiji (50). CD8+ and CD4+ T cells were counted manually (in triplicate) in fields of 650µm2, including the epidermis, dermal-epidermal junction and the upper dermis (51).

Data and statistical analysis: Comparison of T-cell count and density as well as number of T-cell receptor-β chain CDR3 clones between time points, cell populations, and blood/biopsy sites was performed by paired Wilcoxon signed-rank tests. For comparison of T-cell count, the post-vaccination genital biopsies were tested against the arm control and the day 0 baseline biopsy specimen. For comparison of TCR CDR3 clonotypes, genital biopsy time points were compared against corresponding arm biopsy time points. To compute fold change in abundance over time when clonotypes were not present at both time points, a minimal abundance level of 1 copy was assigned to absent clonotypes. *TRA/TRB* sequence data was exported from the Adaptive Biotechnologies platform and analyzed offline. Non-productive sequences and those with inserted stop codons were excluded from analysis. Analyses were performed using SAS 9.4 (SAS institute), Python 3.6.5 and R 3.4.1 (R Core Team). Statistical significance was defined as a two-sided p value ≤ 0.05.

RESULTS

Natural history of the TRB repertoire during HSV-2 reactivation and healing in two individuals

Two persons with symptomatic HSV-2 participated in a natural history study of TRB repertoire sequencing from blood and skin biopsies, not involving therapeutic vaccination (**Fig 1a**). We have previously shown that massive numbers of CD4 and CD8 T cells infiltrate the skin during symptomatic HSV-2 genital lesions, and a smaller, more stable population persists during clinical quiescence (30–32). To establish how TCR repertoires in PBMCs and HSV-2-affected genital skin vary and remain unique or shared over time, we compared the TRB repertoire of skin and blood during an active HSV-2 lesion and at 2-8 weeks post healing (wph) in two persons (**Fig. 1b**). TRB repertoires were obtained from gDNA sequencing, where the number of copies of a specific TRB sequence is representative of the number of cells in which that sequence was detected (33,34). We used clonal tracking to compare the frequency (representing the relative abundance of a specific clonotype within a repertoire which here is either a biopsy specimen or blood sample) of clonotype detection by TRB nucleic acid sequence across samples (34). The Morisita overlap index (mi), a diversity metric used to compare the frequency and distribution of shared sequences in different TCR repertoires, of serial blood samples in these participants during a symptomatic HSV lesion and 8 weeks after healing was 0.92 and 0.98, consistent with substantial shared diversity of the sequential blood samples (**Fig. 1b**).

Comparing unsorted peripheral blood TCR repertoires with that from lesion-area skin in these two participants (**Fig. 1c,d)**, 8.9% and 7.4% of TRB sequences at the time of the lesion, or 11.5% and 14.6% at 8 wph were also detected in blood, and these tended to be the more highly abundant clonotypes at both time points. Of the clonotypes seen in both blood samples, 32.8%

and 56.2% were also found in lesion skin (in Participants P1 and P2, respectively) (**Fig. 1c,d)**. In comparison, during clinical quiescence at 8wph, a smaller fraction of these overlapping clonotypes were also observed in skin, 10.4% and 11.9%, and many of the highly abundant clonotypes in PBMCs were not detected in skin at all (**Fig. 1c,d**). These observations are consistent with antigen-non-specific influx and egress of non-resident T cells occurring during inflammation associated with a skin lesion (28). Indeed, 503 of the TRB CDR3 sequences in the lesion biopsies from these two persons were associated with CMV, EBV, or influenza specificity in a published TCRβ database (35) compared to only 43 of the sequences at 8wph. One hundred seventeen of 503 (37%) from the lesion and 34 of 43 (90%) from 8 wph were also found in blood. In summary, TCR repertoire overlap in serial PBMC samples and between PBMCs and skin during an HSV-2 lesion favored highly abundant clonotypes, consistent with infiltration of T cells from the blood into skin during an HSV-2 lesion. In contrast, during quiescence PBMC-based clonotypes constituted a smaller fraction of the skin-based TCR repertoire.

We next compared the consistency of the TRB repertoire over time in skin during clinical quiescence, and the stability of the TRB repertoire after healing. Shared clonotypes represented a small fraction of the total number of clonotypes at the time of the lesion (5.9% and 3.9%), but a sizable proportion of clonotypes detected at 8wph (31.0% and 50.6%) (**Fig. 1e,f**). Likewise, serial biopsies of healing skin (2, 4, and 8wph) showed a substantial fraction of shared clonotypes were present in multiple other biopsies (47-85% of post healing biopsies) (**Fig 1f**). As in **Fig. 1b,d**, heat mapping in **Fig. 1e** represents the abundance of clonotypes that were also detected in blood. A comparison of differentially abundant clonotypes at the lesion and 8wph

time points, using the beta-binomial calculation that tests the change in frequency of TCR sequences in a repertoire in comparison to what would be expected in serial blood samples (36), shows the stability of the PBMC TRB repertoire over time. In comparison, in skin there are multiple clonotypes that are at significantly greater abundance at either the lesion or 8wph time points. Interestingly, all 18 differentially abundant clonotypes (blue dots) at the lesion time point were also detected in PBMC samples (**Fig. 1g**). Similarly, of the 53 differentially abundant clonotypes from the 8wph, 28 were detected in all quiescent skin samples. Together these data show that, in skin, the TRB repertoire during quiescence represents a relatively stable population with a sizable proportion of clonotypes detected in multiple sequential samples. We hypothesized that biopsies during these quiescent time points would thus be enriched for HSV-specific resident memory T cells (TRM).

Vaccination does not alter T cell abundance or localization at sites of HSV-2 reactivation

Nine persons between the ages of 32 and 54 years with a known history of symptomatic HSV-2 (median duration 11.9 years) were enrolled in a three-dose Phase 1 trial of HSV529, a replication-deficient whole virus immunotherapeutic HSV-2 vaccine candidate (**Fig. 2a, Supplementary Tables 1,2**) (clinicaltrials.gov, NCT02571166). Vaccine doses were given at days 0, 30, and 180 and biopsies were performed at days 0, 10, 30, 40, 180, and 190 (**Fig. 2a**). Seven participants completed the entire three-dose, seven-biopsy study protocol; two completed biopsies through day 40 (2 vaccine doses).

T cell immunofluorescence showed that vaccination was not associated with an increase in CD4+ or CD8+ T-cell number (**Fig. 2b,c**) at the lesion site. We also did not observe differences in CD4+ or CD8+ spatial localization at either the lesion site or arm (**Fig. 2d,e)**. Interestingly, the number of CD4 T cells in the arm was significantly higher after dose 1 and 2 (day 10 and 40) compared to prior to vaccination (14.0 vs. 40.0 and 49.8 cells/mm2, $p = 0.02$ and 0.01, respectively), but the number of CD8 T cells did not change significantly. The density of total CD4 and CD8 T cell infiltration was lower in the arm at enrollment compared to the lesion area at day 0 (**Fig. 2b,c**). Four participants had a lesion fewer than three months prior to enrollment in the vaccine trial and these were biopsied. All lesion biopsies demonstrated the massive lymphocyte infiltration typically associated with symptomatic reactivation (**Fig. 2b,c,f**).

<u>TCR repertoire in lesion-area skin is altered over the course of vaccination with HSV529</u>

TRB sequencing from baseline lesion site biopsies taken just before vaccination (day 0) identified a median of 1,966 unique clonotypes and 52 clonotypes identified at >4 copies per participant (**Fig. 2g, h**). Vaccination did not result in a significant increase in the median number of unique clonotypes in the lesion area per participant, the number of clonotypes detected at >4 copies or in the total number of TRB β CDR3 copies detected per participant by paired Wilcoxon test. Comparison of the TCR repertoire in control (arm) biopsies over time revealed a similar stability of T-cell density and clonality, both of which were lower than that of genital skin. More clonotypes were detected at >4 copies in HSV lesion sites than in the arm overall and at two of three sampled timepoints (day 10 and 190), $p < 0.01$, but not at day 40 (**Fig. 2h**). TCR repertoire clonality, defined as the inversion of Shannon entropy (a comparative measure

of the number and frequency of unique TRB sequences in each sample) (37), was greater in lesion site than arm biopsies at day 10 ($p = 0.03$), but did not change in the lesion site after any of the three vaccinations (**Fig 2i**).

Vaccination elicited HSV-2-reactive CD4s in blood and increased the number of these clonotypes detected in lesion area skin

HSV-2-reactive CD4+ T-cell clonotypes from PBMCs before and after vaccination were identified in all nine participants by IFNγ and IL-2 co-expression by intracellular cytokine staining (ICS+) after incubation with UV-inactivated HSV-2 (**Supplementary Fig. 1**). At day 0, a median of 30 unique clonotypes per participant were identified (range 25-51). After vaccination, the median number of unique HSV-2-reactive clonotypes increased by 8-fold to a median of 237 clonotypes/participant (range 46-1360, unpaired Wilcoxon $p = 0.002$ excluding participant 4, whose cells underwent in vitro expansion prior to sequencing). Almost all the 233 HSV-2-reactive clonotypes found in PBMC at day 0 in the nine participants were detected at a single copy, whereas at day 10, clonotypes were found at >1 copy in 6 of 9 participants. The low copy number of each unique T cell sequence, particularly from day 0, is not unexpected because HSV-2-reactive T cells were not expanded in vitro prior to sequencing (not including participant 4) and represented only a few hundred cells at day 0 (range 165-7,696, median 642 ICS+ cells, or range 0.05-2.5%, median 0.2% of sorted CD4+ T cells at day 0, compared to a range of 343-13,161, median 5059 ICS+ cells, or 0.3-3.3%, median 0.5%, sorted CD4+ T cells at day 10). The percent ICS+ sorted CD4+ T cells increased from day 0 to day 10, but not significantly ($p = 0.05$ by unpaired Wilcoxon, not including participant 4) (**Supplementary Fig. 1**).

Of 205 HSV-2-reactive clonotypes detected in PBMCs at day 0, five (2.4%) were also detected in blood at day 10 (**Fig. 3a**). Sixteen of 205 (7.8%) were detected in any skin biopsy, 7 of those were at day 0 and 8 were at day 10, and none were detected in skin from 4 of 7 participants after day 10 (**Supplementary Fig. 2**). Of the 3285 HSV-2-reactive clonotypes detected at day 10, five (0.1%) had been detected in blood at day 0 (**Fig. 3b**), but 447 (13.6%) were detected in any skin biopsy. This included 203 that were detected in skin (but not blood) at day 0. **Fig. 3c** shows these clonotypes detected in PBMCs at day 10 and their appearance in serial skin biopsies from the site of HSV-2 reactivation and the arm. In the arm, the number of CD4+ T cells increased from day 0 to day 10 and stayed elevated at day 40 (**Fig. 2a**). Clonotype data from arm controls was only available at day 0 from 4 participants, but overlap between either day 0 or day 10 HSV-2-reactive clonotypes from blood was low in these 4 (0-5 clonotypes per participant) (**Supplemental Fig. 2, Fig. 3c,d**). At post-vaccination time points in the arm the number of HSV-2 reactive clonotypes ranged from 0-25 clonotypes per person.

In lesion-area skin, the total number of clonotypes also detected in blood increased from 16 from blood at day 0 to 447 in blood at day 10, but most of these overlapping clonotypes in blood at day 10 had been observed in skin at day 0. The percentage of HSV-2 reactive clonotypes from day 10 PBMCs present in skin at any time point that had also been observed in skin prior to vaccination at day 0 represented a majority at each time point, ranging from 52.7% at day 30 to 63.9% at day 180. The number of HSV-2-reactive CD4+ T cell clonotypes from blood at day 10 detected in skin was significantly higher than those from PBMCs at day 0 (median 199

vs 7.5 clonotypes per time point, p = 0.03). The percentage of the skin clonotypes that these day 10 ICS+ T cells represented increased from day 10 to day 180 and 190 by paired Wilcoxon (medians 0.9%, 1.1%, 1.6%, p = 0.03 (d10 vs d180), 0.01 (d10 vs d190)) (**Fig. 3d**), though there were 3 participants in whom blood-overlapping TRB sequences represented <1% of sequences at any biopsy. Vaccination was therefore seen to increase the number of HSV-reactive CD4+ clonotypes in blood and their detection in tissue, and the majority of these overlapping clonotypes had been observed in skin prior to initiation of vaccination and persisted in the tissue throughout the duration of the study. Despite the increase in detection in day 10 PBMCs, clonotypes overlapping with PBMCs over all participants still represented a very small percentage of the total number of detected clonotypes in lesion-area skin.

TCR repertoire analysis of all CD4+ T clonotypes responding to HSV-2 antigen detected in the day 10 PBMC sample at ≥6 copies from participant 4, ranked by whether they were present prior to or after vaccination and the abundance of those clonotypes in skin is shown in **Fig. 3e**. Here it is visible that clonotypes detected in blood, even with in vitro expansion to try to increase the yield of sequencing, were detected infrequently and not at high abundance in skin. All HSV-2 reactive CD4+ T cell clonotypes from PBMCs and their relative abundances in skin are shown in **Supplementary Fig. 3**.

Persistence and expansion of skin-based clonotypes

As vaccination did not substantially change the total number of skin-based clonotypes in the lesion area site, the percentage of skin-based clonotypes that could be determined to be HSV-2

reactive by overlap with blood clonotypes was quite low, and because these ICS+ cells did not appear to be the clonotypes of greatest abundance in skin, we next looked to characterize the skin-based repertoire over time and to determine whether the relative abundance of clonotypes in the skin-based repertoires changed over the course of vaccination. To identify clonotypes of interest, we identified and ranked the skin-based clonotypes that increased the most (≥6 fold increase in number of copies) after the first vaccine dose (between day 0 to day 10) and examined their durability in serial biopsies from lesion area skin and detection in serial biopsies from the arm and their detection in HSV-2-reactive CD4+ T cells from PBMCs. Heat maps in **Fig. 4** illustrate number of copies in serial biopsies of clonotypes identified prior to vaccination that increased ≥6-fold after dose 1 (prevalent clonotypes) (**Fig. 4a,c, e left**) or were newly identified at ≥6 copies at day 10 after dose 1 (elicited clonotypes) (**Fig. 4b,d, e right**) in two participants, in comparison to the number of these clonotypes detected in the blood or the arm. (Cells from participant 4 that underwent in vitro expansion are shown with $). All other participants are shown in **Supplementary Fig. 4**. In all participants, there was more expansion (by number of clonotypes increasing by ≥6 fold) in the lesion area biopsies from day 0 to day 10 than in the arm biopsies from day 10 to 190 and day 40 to 190 by paired Wilcoxon test ($p = 0.04$, $p = 0.02$), though not from day 10 to 40. There were two participants in whom an especially large number of expanding clonotypes were detected after dose 1 (participant 2 and 4), and one who had more expansion after dose 2 (participant 6). For example, Pt 4 had 31 clonotypes detected in the day 0 biopsy that increased ≥6-fold by day 10: several clonotypes increased >20-fold and one expanded from 3 to 285 copies (>80 fold) (**Fig. 4a**). This same participant had 97 elicited clonotypes that were detected at ≥6 copies at day 10, and 38 of

those were detected at ≥10 copies (**Fig. 4b**). Over all participants, after the first vaccination, 14.0% of prevalent clonotypes on average were at ≥6 copies (range 11-429 clonotypes/person) compared to 0.89% of elicited clonotypes (range 0-146 clonotypes/person) (paired Wilcoxon p = 0.004) (**Fig. 4e**). Of all prevalent clonotypes, 5% on average expanded ≥6-fold from day 0 to day 10 (range 1-198 clonotypes/person), which was also significantly greater than the 0.89% percent of elicited clonotypes mentioned above (p = 0.04). In summary, clonotypes present in genital skin at day 0 (prevalent clonotypes) were more likely than elicited clonotypes to increase in copy number after the first vaccination (vs be detected at a high copy number after first vaccination) and were more often detected in subsequent biopsies than clonotypes that were first detected after dose 1.

Prevalent clonotypes were more persistent in tissue than elicited clonotypes, based on the number of biopsy samples in which they were detected. For example, in Pt 4, 22 of the 36 (73%) prevalent clonotypes that expanded ≥6-fold were detected at all subsequent timepoints through day 190 (**Fig. 4a**). In comparison, only 35 of 97 (36%) of the elicited clonotypes were similarly persistent. A similar pattern was seen in all participants: of all 3949 clonotypes detected in a majority of biopsies from any participant, 3141 were prevalent clonotypes. A median of 9.3% of prevalent clonotypes were present in more than half of genital skin biopsies, compared to 0.7% of elicited clonotypes (p = 0.004 by paired Wilcoxon) (**Fig. 4f**). Conversely, 97.6% of elicited clonotypes were found in two or fewer biopsies, compared to 85.5% of prevalent clonotypes (p = 0.004).

Figs. 4c, d display the clonotypes that expanded ≥6-fold from day 30 to day 40 pre and post dose 2 (prevalent, **Fig. 4c**) or were detected at >6 copies at day 40 after not being present prior to vaccination (elicited, **Fig. 4d**) in two participants, others are shown **Supplementary Fig. 3 and 4.** Participant 6 was the only participant in whom greater expansion was detected after dose 2 than dose 1. In all participants, 295 clonotypes increased in copy number after dose 2. Of those, 72 expanded ≥6 fold over the first dose and 11 expanded ≥6 fold over the second (day 30 to day 40); only one clonotype (in participant 6) expanded ≥6 fold over both doses. Over all participants, more expansion was detected after dose 1 than over the whole 6-month biopsy series or over the ten days before and after doses 2 and 3.

Disparity between skin and PBMC clonotypes

In this study with serial blood and skin samples from 9 participants, by TCR repertoire sequencing the populations of T cells in the skin and blood shared few clonotypes. Among the groups of TCRs identified above as clonotypes of interest in skin: those expanding ≥6 fold after the first vaccine dose, those appearing at ≥6 copies after the first vaccine dose, and those that were detected in more than half of all lesion-area biopsies, still a small minority were detected in PBMCs. Over all samples 0.7% of skin-based TRB sequences were detected among HSV-2-reactive CD4+ T cells from PBMCs (463 of 62,451), which reflects 13% of PBMC-detected HSV-2-reactive CD4+ T cells (463 of 3490). The day 10 blood sample captured 4% of expanded (increased by ≥6 fold after dose 1) or highly elicited (detected at ≥6 copies at day 10) tissue-based clonotypes (22 of 528): 10 prevalent and 12 elicited clonotypes from 2 individuals. It also captured 3.7% (149 of 3949) of clonotypes resident in skin i.e. clonotypes detected in a majority

of skin biopsies (either >3/6 or >2/4). The blood sample at day 0 did not capture any clonotypes expanded or elicited at ≥6 copies and captured only 7 (0.2%) of skin resident clonotypes.

We next looked to determine whether clonotypes of interest were more likely to be detected in PBMCs. As was suggested in our natural history analysis, clonotypes at a greater frequency in skin were more likely to be seen in PBMCs, but these still represented a small percentage of the skin-derived T-cell population. A median of 4.6% of clonotypes at ≥6 copies in the lesion-area biopsy at day 10 were detected in blood at day 10, compared to 0.9% of clonotypes at <6 copies (Wilcoxon $p = 0.035$). If overlap was compared by amino acid sequence in lieu of nucleic acid sequence, the results were similar (4.7% vs 0.8%, $p = 0.042$). This represented enrichment in the blood for more highly detected tissue-based clonotypes – at day 10, 15.6% of blood-detected HSV-2-specific clonotypes (55 of 256 clonotypes) were seen in tissue at ≥6 copies, whereas only 3.6% of all tissue-detected clonotypes were seen at ≥6 copies (1025 of 20,428 total clonotypes among all participants at day 10). Whether a clonotype was seen to expand in tissue after vaccination was not related to whether a clonotype was more likely to be detected in blood, whether defined as expansion ≥6 or ≥3 fold over day 0 ($p = 1$ by paired Wilcoxon), or if defined as expansion vs contraction from day 0 to day 10 ($p = 0.56$ by paired Wilcoxon). In summary, vaccination enhanced detection in blood of a small percentage of skin-resident HSV-2-reactive clonotypes in all participants. Both highly abundant and resident skin clonotypes were enriched among HSV-2 reactive CD4+ T cells from peripheral blood at day 10. Clonotypes of identified to be of interest based on expansion or elicitation after vaccination, however, were not enriched in these cells.

Shift in TRA/TRB clonotype oligodominance after vaccination in two participants

To further investigate changes in TCR repertoires after vaccination, we evaluated the distribution of V-J usage within each participant's TCR repertoire. Vaccination resulted in a shift of V-J usage in two of the nine participants after the first dose (Pts 4 and 8). In participant 8, a relatively uncommon V-J combination BV06-06, BJ02-01 increased in abundance ~50-fold from day 0 to day 10 but receded by day 30. Similar oligodominance was not observed in the arm biopsies and none of these combinations in skin were abundant in PBMCs (**Supplementary Fig. 6a,b**). In participant 4, by sequencing archived samples we found that prior to vaccination a highly oligodominant V-J combination had been dominant for more than two years, and a novel oligodominant V-J combination became dominant at day 10 and remained so throughout the remainder of the trial. Prior to vaccination (day 0 and two years before the vaccine trial) in Pt 4, the most dominant V-J gene combination was AV21-01 AJ33-01 (blue) and BV07-09 BJ02-01. After vaccination, oligodominance switched to AV25-01, AJ15-01, red and BV14-01 BJ02-05, blue, and this remained the most abundant V-J combination at day 190. **Fig. 5a** illustrates the oligoclonal pattern by TRAV/J genes of the most prevalent TCR clonotypes at day 0 and day 10 in Pt 4. TRBV/J gene usage over time in all participants are shown in **Supplementary Fig. 5a**. The specific CDR3 sequences and abundance of TRA and TRB sequences comprising the oligodominant "spikes" in Pt 4 are shown in **Fig. 5b**. This shifted, oligodominant VJ combination remained dominant through all subsequent biopsies.

We next wanted to determine whether the most abundant post-vaccination TCRαβ combination in participant 4 (AV25-01, AJ15-01 CAEYQAGTALIF, BV14-01 BJ02-05 CASSQGETQYF) was HSV-2-specific. Because it was not detected in blood at day 10 by TRB sequencing or AIM-based isolation of HSV-2-reactive T cells from PBMCs, a synthetic TCR with this combination was expressed in a CD4-expressing Jurkat-based cell line with a NR4A1-mNeonGreen reporter system (GenBank accession numbers MZ821077, MZ821078). NR4A1, also known as Nur77, is activated upon binding of the TCR to ligand. The transduced cell line showed reactivity in response to whole HSV-2 presented by autologous antigen presenting cells (APC), indicating HSV-2-specificity (**Fig 5c**). Specificity was refined by showing reactivity to a single HSV-2 protein, VP22, encoded by *UL49*, and a single VP22 peptide corresponding to residues 81-93 (ARPRRSASVAGSH) (**Supplementary Fig. 6a**). To determine if this TCR had the characteristics of TCRs used by CD4+ T cells, we examined inhibition of activation of the reporter Jurkat line by HLA class II loci-specific blocking antibodies. A monoclonal antibody that blocks HLA-DP, but not those that block HLA-DR or DQ, was able to prevent reporter cell activation (**Supplementary Fig. 6b**). Together with recognition of killed viral antigen, these data support that this TRA/TRB pair originated in a CD4+ T cell, indicating that vaccination elicited HSV-specific tissue-based CD4+ T cells.

<u>Mucosal-associated invariant T (MAIT)-like TRA sequences are detectable in HSV lesion site skin but do not show expansion after vaccination</u>

To discern whether a proportion of the skin-based TCR repertoire may represent MAIT cells, as defined by TRA chains utilizing TRAV 01-02 and TRAJ families 12, 20, or 33, we performed TRA

sequencing of biopsies from Pts 4 and 2 (**Supplementary Fig. 7a)**. Overall, potentially MAIT-like cells in both participants represented approximately 2% (0.9-2.6%) of the identified TRA sequences in HSV lesion site and control biopsies and did not expand or contract over time with vaccination (**Supplementary Fig. 7b,c)**. Therefore, this vaccine does not appear to specifically modulate skin-based MAIT-like cells.

Mapping HSV-2 specificity of clonotypes detected in both PBMCs and skin biopsies

To explore the antigenic specificity of clonotypes that were shared in the blood and skin compartments in participant 4, we evaluated CD4+ T cells reactive to HSV-2 from day 10 PBMCs by single cell sorting, TRA/TRB sequencing, and fine specificity determination (**Supplementary Fig. 8**). HSV-2 reactivity was determined by expression of CD137 (4-1BB) by memory T cells after activation through TCR by UV-HSV-2, yielding live, antigen-reactive cells for single-cell cloning directly *ex vivo* (21). Among 192 clones generated from CD4 cells with high CD137 expression after stimulation with UV-HSV-2, 190 expressed IFN-γ in response to whole HSV-2 antigen, suggesting highly efficient enrichment of HSV-2 reactive clones (**Supplementary Fig. 8a,b**). Paired TRA/TRB sequencing yielded a single productive TRB and either one or two productive TRA CDR3 sequences in 160 of these clones (**Supplementary Fig. 8c**). Of these 160, we selected 16 clones that had perfect TRB nucleotide sequence matches in genital skin and had the characteristics of clonotypes of interest – either expanding ≥4 fold after the first dose or were identified at ≥4 copies at day 10. **Fig. 6a** outlines the TRB sequences, number of copies detected in skin and TCR specificity from all 16 clones. To further validate that the TCRs represented classical virus-specific CD4 T cells, we determined their viral protein-level specificity using a

library of all curated HSV-2 proteins (38). Reactivity was observed to proteins encoded by genes *RL2, UL11, UL22, UL23, UL39*, and *US6,* among others, indicating that among these overlapping clonotypes antigenic specificity did not seem to be related to their detection in both compartments. A representative example of HSV-2 protein UL11 specificity is shown in **Fig. 6b**. This also confirmed HSV-2-specificity of 16 clonotypes in participant 4 that were observed to either expand from day 0 to day 10 or were newly detected in tissue after dose 1 at ≥4 copies; clonotypes identified as clonotypes of interest. Therefore, in this participant vaccination induces broad CD4+ T cell reactivity in the skin at a site of previous HSV-2 reactivation.

Discussion

Our study reveals several novel observations pertinent to immunotherapeutic vaccines or systemic immunotherapies for infectious, and likely also malignant diseases. Immunization with a recombinant, replication-defective vaccine delivered intramuscularly in the arm elicited an oligoclonal expansion of HSV-specific responses in blood and skin near the genital region to a varying extent in these 9 participants. This included skin-resident clones present at the time of vaccination as well as clonotypes not detected before vaccination. TCR clonotypes that increased in abundance after vaccination in both blood and skin and persisted in skin over time were most often detectable in skin prior to vaccination. While vaccination led to an increase in detection in blood of resident and highly abundant clonotypes from skin, these represented a small minority of the total skin clonotypes and clonotypes of interest. Our findings are compatible with our current understanding of the immune response to chronic infection with HSV-2: there is a population of skin-resident T cells that are located at the site of reactivation

and are poised to respond to viral challenge as it occurs (28,30,31). Hence, for a sustained response, it is tissue-based clonotypes to which immunotherapy must be directed.

The uniqueness and persistence of the skin-resident population is shown most strikingly in participant 4, in whom TCR repertoire sequencing was able to be performed on samples from two years prior to the present study. An oligoclonal population (>10% of TCR clonotypes derived from the same VJ combination) was detected in genital region biopsies and was not present in the arm or in HSV-reactive CD4+ T cells from PBMCs. A switch in the immunodominant oligoclonal "swarm" of TCRs occurred after the first vaccine dose and was sustained for the full six months of this study. By creation of a synthetic TCR, we were able to confirm that this dominant T-cell clonotype originated from an HSV-2-reactive CD4+ T cell and its specificity was mapped to UL49. Vaccination, including repeated boosting doses of vaccine, was not associated with an increase in the total cell population at the site of HSV-2 reactivation as measured by T-cell density, and indeed, boosting did not appear to enhance responses described here after dose 1 by T-cell count or clonal tracking. However, in all participants, selective increases in clonotypes were observed and detection of shared HSV-2-reactive TRB sequences increased after the first vaccine dose, albeit expansion varied considerably by participant. Determinants of such variability absolutely require further evaluation. These data indicate that immunogenicity studies of immunotherapeutic vaccines should carefully assess alterations in the TCR repertoire of the pathogen under study and not necessarily a total quantitative increase in antigen-specific T cells.

Within person TRB nucleotide sequence overlap with defined HSV-2 reactive clonotypes from PBMCs was used here as a surrogate indicator of HSV-2 specificity of tissue-based TRB

sequences. This mechanism undoubtedly misses a large proportion of tissue-based HSV-2-specific T cells, such as the non-blood clonotype shown to be HSV-2-specific when expressed in a reporter system, but the true extent of HSV-2 specificity among tissue-resident T cells has not been defined. Alternative methods to expand the capacity to determine the specificity of tissue-based T cell clonotypes are in development, but clonal tracking is one novel method to expand the capacity to define T cell specificity into difficult to reach compartments.

Perhaps the most provocative and unequivocal observation from our study is that HSV-2-reactive CD4+ T-cell clonotypes that were detected in PBMCs both prior to and after vaccination, the population that would typically be the focus of an evaluation of vaccine efficacy and of a correlate of protection, represented a tiny fraction of the clonotypes found in skin. HSV-2-reactive CD4 T cell sampling from PBMCs as performed here did not detect more than 95% of clonotypes in the genital region, including the vast majority of the most abundant and persistent clonotypes. Studies to date that have evaluated T-cell responses of persons naturally infected with HSV-2 or receiving vaccination with candidate vaccines have utilized PBMC sampling to evaluate vaccine efficacy or correlates of protection (12,16,39). The results from the current study suggest that this sampling of convenience may be limited, or even misleading.

Some of the lack in overlap between skin and CD4 T cells from PBMCs is magnified by the ability to select for CD4+ T cells with HSV-2 specificity from PBMC samples, which was not feasible for skin biopsies. Altogether, even when selecting for those TCR clonotypes in greatest abundance in skin where overlap with PBMCs seems most likely, there was little representation in the HSV-2-enriched CD4+ T-cell samples. In a chronic viral disease for which an effective

vaccine has not been found after many years of trials, we wonder whether the focus on responses in PMBCs may partly explain previous failures. Our findings suggest that the inclusion of skin-based responses in the design of immunotherapeutic vaccines with a skin-based target may provide novel insights and perhaps bring an effective vaccine for HSV-2 and other chronic infections closer to reality. This study has shown conceptually that therapeutic targeting of T cells resident in genital skin sites by immunotherapeutic vaccination is possible.

List of Supplementary Materials:
Table S1. Procedures and study visits.
Table S2. Demographic characteristics of study participants.
Figure S1. Schema of selection procedures for HSV-2-reactive CD4+ T cells from PBMCs and number and proportion of IFNg/IL-2+ T cells submitted for sequencing.
Figure S2. Number of PBMC-detected HSV-2-reactive CD4+ T cell sequences detected in blood at day 0 and at any time point in the skin at the site of HSV-2 reactivation and the arm.
Figure S3. All HSV-2-reactive clonotypes detected in PBMCs that were also detected in skin at any time point.
Figure S4a. Clonal tracking of skin-based clonotypes ranked by fold change in abundance of copies from day 0 to day 10 in each participant. 4b. Clonotypes from all participants ranked by fold change over second vaccination (day 30 to day 40), to rank fold change undetected clonotypes were given a value of 1. Prevalent and elicited are defined by presence or absence of detection at day 0.
Figure S5. Relative use of Vβ and Jβ genes in TCRβ sequencing from HSV lesion site biopsies by participant and study day in comparison to those seen in HSV-2 reactive CD4+ T cells from PBMCs ("blood") and arm biopsies.
Figure S6. Protein (a) and peptide-level (b) specificity in the synthetic TCR from participant 4 and testing of HLA-II blocking by monoclonal antibodies against HLA-DP, DQ and DR (c).
Figure S7. V-J combinations highly suggestive of MAIT cell derivation represent a small minority of the TCRα clonotypes detected in a single individual over time.
Figure S8. Identification of HSV-2-reactive CD4+ T cells from frozen PBMCs from participant 4 for determination of fine specificity, confirmation of reactivity and bulk sequencing results.
Supplementary Methods

References:

1. Looker KJ, Magaret AS, Turner KME, Vickerman P, Gottlieb SL, Newman LM. Global

estimates of prevalent and incident herpes simplex virus type 2 infections in 2012. PLoS One. 2015;10(1):1–23.

2. Looker KJ, Elmes JAR, Gottlieb SL, Schiffer JT, Vickerman P, Turner KME, et al. Effect of HSV-2 infection on subsequent HIV acquisition: An updated systematic review and meta-analysis. Lancet Infect Dis [Internet]. 2017;3099(17):1–14. Available from: http://linkinghub.elsevier.com/retrieve/pii/S147330991730405X

3. Looker KJ, Magaret AS, May MT, Turner KME, Vickerman P, Newman LM, et al. First estimates of the global and regional incidence of neonatal herpes infection. Lancet Glob Heal [Internet]. 2017;5(16):1–10. Available from: http://dx.doi.org/10.1016/S2214-109X(16)30362-X

4. Posavad CM, Koelle DM, Shaughnessy MF, Corey L. Severe genital herpes infections in HIV-infected individuals with impaired herpes simplex virus-specific CD8+ cytotoxic T lymphocyte responses. Proc Natl Acad Sci U S A [Internet]. 1997;94(19):10289–94. Available from: http://www.pubmedcentral.nih.gov/articlerender.fcgi?artid=23355&tool=pmcentrez&rendertype=abstract

5. Bernstein DI, Wald A, Warren T, Fife K, Tyring S, Lee P, et al. Therapeutic vaccine for genital herpes simplex virus-2 infection: Findings from a randomized trial. J Infect Dis. 2017;215(6):856–64.

6. Van Wagoner N, Koltun W, Lucksinger G, Warren T, Tyring S, Bernstein D, et al. GEN-003 phase 2 interim results: Therapeutic vaccine for genital herpes significantly reduces viral shedding and genital lesions. Open Forum Infect Dis. 2015;2(Supplemental 1):898.

7. Wald A, Warren T, Fife K, Tyring S, Lee P, Van Wagoner N, et al. Therapeutic HSV-2 vaccine (GEN003) results in durable reduction in genital lesions at 1 year. Open Forum Infect Dis. 2014;1(Suppl 1):S55–6.

8. Straus SE, Corey L, Burke RL, Savarese B, Barnum G, Krause PR, et al. Placebo-controlled trial of vaccination with recombinant glycoprotein D of herpes simplex virus type 2 for immunotherapy of genital herpes. Lancet. 1994;343:1460–3.

9. Boukhvalova M, McKay J, Mbaye A, Sanford-Crane H, Blanco JCG, Huber A, et al. Efficacy of the herpes simplex virus 2 (HSV-2) glycoprotein D/AS04 vaccine against genital HSV-2 and HSV-1 infection and disease in the cotton rat Sigmodon hispidus model. J Virol [Internet]. 2015;89(19):9825–40. Available from: http://jvi.asm.org/lookup/doi/10.1128/JVI.01387-15

10. Belshe RB, Heineman TC, Bernstein DI, Bellamy AR, Ewell M, Van Der Most R, et al. Correlate of immune protection against HSV-1 genital disease in vaccinated women. J Infect Dis. 2014;209(6):828–36.

11. Straus SE, Wald A, Kost RG, McKenzie R, Langenberg AGM, Hohman P, et al. Immunotherapy of recurrent genital herpes with recombinant herpes simplex virus type 2 glycoproteins D and B: results of a placebo-controlled vaccine trial. J Infect Dis [Internet]. 1997;176(5):1129–34. Available from: http://www.ncbi.nlm.nih.gov/pubmed/9359709

12. Koelle DM, Magaret A, McClurkan CL, Remington ML, Warren T, Teofilovici F, et al. Phase I dose-escalation study of a monovalent heat shock protein 70-herpes simplex virus type 2 (HSV-2) peptide-based vaccine designed to prime or boost CD8 T-cell responses in HSV-

naive and HSV-2-infected subjects. Clin Vaccine Immunol. 2008;15(5):773–82.

13. Wald A, Koelle DM, Fife K, Warren T, LeClair K, Chicz RM, et al. Safety and immunogenicity of long HSV-2 peptides complexed with rhHsc70 in HSV-2 seropositive persons. Vaccine [Internet]. 2011;29(47):8520–9. Available from: http://dx.doi.org/10.1016/j.vaccine.2011.09.046

14. Dropulic LK, Oestreich MC, Pietz HL, Laing KJ, Hunsberger S, Lumbard K, et al. A randomized, double-blind, placebo-controlled, phase 1 study of a replication-defective herpes simplex virus 2 vaccine, HSV529, in adults with or without HSV infection. J Infect Dis. 2019;20892(Xx):1–11.

15. Ouwendijk WJD, Laing KJ, Verjans GMGM, Koelle DM. T-cell immunity to human alphaherpesviruses. Curr Opin Virol [Internet]. 2013;3(4):452–60. Available from: http://dx.doi.org/10.1016/j.coviro.2013.04.004

16. Laing KJ, Magaret AS, Mueller DE, Zhao L, Johnston C, De Rosa SC, et al. Diversity in CD8+ T cell function and epitope breadth among persons with genital herpes. J Clin Immunol. 2010;

17. Koelle DM, Abbo H, Peck A, Ziegweid K, Corey L, The S, et al. Direct recovery of herpes simplex virus (HSV) -specific T lymphocyte clones from recurrent genital HSV-2 lesions. J Infect Dis. 1994;169(5):956–61.

18. Koelle DM. Expression cloning for the discovery of viral antigens and epitopes recognized by T cells. Methods. 2003;29(3):213–26.

19. Jing L, Schiffer JT, Chong TM, Bruckner JJ, Davies DH, Felgner PL, et al. CD4 T-cell memory responses to viral infections of humans show pronounced immunodominance

independent of duration or viral persistence. J Virol [Internet]. 2013;87(5):2617–27. Available from: http://www.pubmedcentral.nih.gov/articlerender.fcgi?artid=3571405&tool=pmcentrez&rendertype=abstract

20. Moss NJ, Magaret A, Laing KJ, Kask AS, Wang M, Mark KE, et al. Peripheral blood CD4 T-cell and plasmacytoid dendritic cell (pDC) Reactivity to herpes simplex virus 2 and pDC number do not correlate with the clinical or virologic severity of recurrent genital herpes. J Virol [Internet]. 2012;86(18):9952–63. Available from: http://jvi.asm.org/cgi/doi/10.1128/JVI.00829-12

21. Jing L, Haas J, Chong TM, Bruckner JJ, Dann GC, Dong L, et al. Cross-presentation and genome-wide screening reveal candidate T cells antigens for a herpes simplex virus type 1 vaccine. J Clin Invest. 2012;122(2):654–73.

22. Sato A, Suwanto A, Okabe M, Sato S, Nochi T, Imai T, et al. Vaginal memory T cells induced by intranasal vaccination are critical for protective T cell recruitment and prevention of genital HSV-2 disease. J Virol [Internet]. 2014;88(23):13699–708. Available from: http://www.ncbi.nlm.nih.gov/pubmed/25231301

23. Schiffer JT, Abu-Raddad L, Mark KE, Zhu J, Selke S, Koelle DM, et al. Mucosal host immune response predicts the severity and duration of herpes simplex virus-2 genital tract shedding episodes. Proc Natl Acad Sci U S A. 2010;107(44):18973–8.

24. Ariotti S, Hogenbirk MA, Dijkgraaf FE, Visser LL, Hoekstra ME, Song J-Y, et al. Skin-resident memory CD8+ T cells trigger a state of tissue-wide pathogen alert. Science [Internet]. 2014;346(6205):101–5. Available from:

http://www.ncbi.nlm.nih.gov/pubmed/25278612

25. Iijima N, Iwasaki A. A local macrophage chemokine network sustains protective tissue-resident memory CD4 T cells. Science. 2014;346(6205):93–8.

26. Shin H, Iwasaki A. A vaccine strategy that protects against genital herpes by establishing local memory T cells. Nature [Internet]. 2012;491(7424):463–7. Available from: http://dx.doi.org/10.1038/nature11522

27. Gebhardt T, Wakim L, Eidsmo L, Reading P, Heath W, Carbone F. Memory T cells in nonlymphoid tissue that provide enhanced local immunity during infection with herpes simplex virus. Nat Immunol. 2009;10(5):524–30.

28. Zhu J, Peng T, Johnston C, Phasouk K, Kask AS, Klock A, et al. Immune surveillance by CD8αα+ skin-resident T cells in human herpes virus infection. Nature. 2013;497(7450):494–7.

29. Gebhardt T, Whitney PG, Zaid A, MacKay LK, Brooks AG, Heath WR, et al. Different patterns of peripheral migration by memory CD4+ and CD8+ T cells. Nature [Internet]. 2011;477(7363):216–9. Available from: http://dx.doi.org/10.1038/nature10339

30. Peng T, Zhu J, Phasouk K, Koelle DM, Wald A, Corey L. An effector phenotype of CD8+ T cells at the junction epithelium during clinical quiescence of herpes simplex virus 2 infection. J Virol. 2012;86(19):10587–96.

31. Zhu J, Koelle DM, Cao J, Vazquez J, Huang M-L, Hladik F, et al. Virus-specific CD8+ T cells accumulate near sensory nerve endings in genital skin during subclinical HSV-2 reactivation. J Exp Med. 2007;204(3):595–603.

32. Zhu J, Hladik F, Woodward A, Klock A, Peng T, Johnston C, et al. Persistence of HIV-1

receptor-positive cells after HSV-2 reactivation is a potential mechanism for increased HIV-1 acquisition. Nat Med. 2009;15(8):886–92.

33. Robins HS, Campregher P V, Srivastava SK, Wacher A, Turtle CJ, Kahsai O, et al. Comprehensive assessment of T-cell receptor beta-chain diversity in alpha-beta T cells. Blood [Internet]. 2009 Nov 5 [cited 2019 Jan 31];114(19):4099–107. Available from: http://www.ncbi.nlm.nih.gov/pubmed/10845939

34. Carlson CS, Emerson RO, Sherwood AM, Desmarais C, Chung MW, Parsons JM, et al. Using synthetic templates to design an unbiased multiplex PCR assay. Nat Commun [Internet]. 2013;4:1–9. Available from: http://dx.doi.org/10.1038/ncomms3680

35. Tickotsky N, Sagiv T, Prilusky J, Shifrut E, Friedman N. McPAS-TCR: A manually curated catalogue of pathology-associated T cell receptor sequences. Bioinformatics. 2017;33(18):2924–9.

36. Rytlewski J, Deng S, Xie T, Davis C, Robins H, Yusko E, et al. Model to improve specificity for identification of clinically-relevant expanded T cells in peripheral blood. PLoS One. 2019;14(3):1–10.

37. Coffey DG. LymphoSeq: Analyze high-throughput sequencing of T and B cell receptors. R Package version 1180. 2020;

38. Johnston C, Zhu J, Jing L, Laing KJ, McClurkan CM, Klock A, et al. Virologic and immunologic evidence of multifocal genital herpes simplex virus 2 infection. J Virol [Internet]. 2014;88(9):4921–31. Available from: http://www.ncbi.nlm.nih.gov/pubmed/24554666

39. Flechtner JB, Long D, Larson S, Clemens V, Baccari A, Kien L, et al. Immune responses

elicited by the GEN-003 candidate HSV-2 therapeutic vaccine in a randomized controlled dose-ranging phase 1/2a trial. Vaccine. 2016;34(44):5314–20.

40. Ashley RL, Militoni J, Lee F, Nahmias A, Corey L. Comparison of Western blot (immunoblot) and glycoprotein G-specific immunodot enzyme assay for detecting antibodies to herpes simplex virus types 1 and 2 in human sera. J Clin Microbiol. 1988;26(4):662–7.

41. Da Costa X, Kramer MF, Zhu J, Brockman MA, Knipe DM. Construction, phenotypic analysis, and immunogenicity of a UL5/UL29 double deletion mutant of herpes simplex virus 2. J Virol. 2000;74(17):7963–71.

42. Dropulic L, Wang K, Oestreich M, Pietz H, Garabedian D, Jegaskanda S, et al. 1345. A replication-defective herpes simplex virus (HSV)-2 vaccine, HSV529, is safe and well-tolerated in adults with or without HSV infection and induces significant HSV-2-specific antibody responses in HSV seronegative individuals. Open Forum Infect Dis. 2017;4(October):S415–6.

43. Dong L, Li P, Oenema T, McClurkan CL, Koelle DM. Public TCR use by herpes simplex virus-2-specific human CD8 CTLs. J Immunol [Internet]. 2010;184(6):3063–71. Available from: http://www.jimmunol.org/cgi/doi/10.4049/jimmunol.0903622

44. Jing L, Ott M, Church CD, Kulikauskas RM, Ibrani D, Iyer JG, et al. Prevalent and diverse intratumoral oncoprotein-specific CD8+ T cells within polyomavirus-driven merkel cell carcinomas. Cancer Immunol Res. 2020;8(5):648–59.

45. Nguyen DN, Roth TL, Li PJ, Chen PA, Apathy R, Mamedov MR, et al. Polymer-stabilized Cas9 nanoparticles and modified repair templates increase genome editing efficiency.

Nat Biotechnol [Internet]. 2020;38(1):44–9. Available from: http://dx.doi.org/10.1038/s41587-019-0325-6

46. Shaner NC, Lambert GG, Chammas A, Ni Y, Cranfill PJ, Baird MA, et al. A bright monomeric green fluorescent protein derived from Branchiostoma lanceolatum. Nat Methods. 2013;10(5):407–9.

47. Ashouri JF, Weiss A. Endogenous Nur77 Is a specific indicator of antigen receptor signaling in human T and B cells. J Immunol. 2017;198(2):657–68.

48. Jing L, Laing KJ, Dong L, Russell RM, Barlow RS, Haas JG, et al. Extensive CD4 and CD8 T cell cross-reactivity between alphaherpesviruses. J Immunol [Internet]. 2016;196(5):2205–18. Available from: http://www.jimmunol.org/lookup/doi/10.4049/jimmunol.1502366

49. Schmitt TM, Aggen DH, Ishida-Tsubota K, Ochsenreither S, Kranz DM, Greenberg PD. Generation of TCRs of higher affinity by antigen-driven differentiation of progenitor T cells in vitro. Nat Biotechnol. 2017;35(12):1188–95.

50. Schindelin J, Arganda-Carreras I, Frise E, Kaynig V, Longair M, Pietzsch T, et al. Fiji: An open-source platform for biological-image analysis. Nat Methods. 2012 Jul 1;9(7):676–82.

51. Diem K, Magaret A, Klock A, Jin L, Zhu J, Corey L. Image analysis for accurately counting CD4+ and CD8+ T cells in human tissue. J Virol Methods. 2015;222:117–21.

Acknowledgements:

The authors would like to express their appreciation to Amanda Woodward and Mindy Miner for their assistance in editing and formatting the final manuscript, and to Khamsone Phasouk and Lei Jin for their laboratory expertise.

Funding: The authors would like to acknowledge funding from the NIH to researchers for salary and research support including K08 AI148588 (ESF), U19 AI113173 (ESF, ASM), P01 AI030731 (CJ, ASM, JZ, DMK, LC), R01 AI042528 (JZ, LC), R01 AI134878 (JZ, LC), P30 CA015704 (core facilities). JT and SG are current employees of Sanofi Pasteur. Sanofi Pasteur provided funding to FHCRC for this investigator-initiated trial. The funder was not involved in the study design, data collection, data analysis, decision to publish, or manuscript preparation.

Author contributions:
Study design: CJ, ASM, JZ, LC
TCR data analysis and bioinformatics: ESF, AL, LJ, ASM, DMK, LC
PBMC-based T cell assays and analysis: LD, LJ, KJL, KB, MO, DMK
Skin biopsy analysis: ESF, AK, JZ
Synthetic TCR specificity: KD, ME, AC
Participant recruitment and clinical guidance: CJ
Statistical analysis: ESF, ASM, LC
Vaccine acquisition and regulatory guidance: JT, SG, LC
Manuscript preparation: ESF, CJ, ASM, KJL, DMK, LC
All authors reviewed and approved of the manuscript.

Competing Financial Interests:
JT and SG are current employees of Sanofi Pasteur.
ASM is a consultant for Cero and AiCuris.
CJ has received institutional research funding to the University of Washington from Sanofi, Genocea, Vical and Gilead and is a consultant to AbbVie and Gilead.
DMK has received research funding from Sanofi Pasteur, Immune Design Corporation, and Admedus Immunotherapy concerning herpes vaccines, has served as a consultant to Biomedical Research Models on herpes vaccines, and is a coinventor on patents owned by the University of Washington involving herpes vaccines.
LC is a coinventor listed on several patents involving potential HSV vaccine development.

Data Availability:
These data will be made available to the public at publication.

Code Availability:
The custom code used for these analyses is archived and available here or at reasonable request from the corresponding author:
https://github.com/alvason/visualizing_Tcell_response_after_HSV2_vaccine

Fig. 1. TCR repertoire in PBMC and biopsies from HSV-2 reactivation sites over time. (**a**) Schematic of natural history biopsy study and procedures. (**b**) Plots of CDR3 clonotypes found in PBMC in Participant P1 (top) and Participant P2 (bottom) at lesion vs. 8wph. (**c**) Venn diagrams show the proportion of clonotypes detected in blood and subsequent skin samples. Heatmap overlay compares TCR overlap with skin at lesion (**b**, red) and skin at 8wph (**d**, blue). (**e**) Plots of CDR3 clonotypes found in skin in Participant 1 (top) and Participant 2 (bottom) during quiescence at 4wph vs. 8wph. Heatmap overlay indicates overlap between the TCR repertoire from skin and PBMC at 8wph. (**f**) Venn diagrams show the proportion of clonotypes detected in skin at lesion vs. later healing time points. (**g**) Evaluation of differentially abundant clonotypes in blood (top) vs skin (bottom) at the lesion vs 8wph time points.

Fig. 2. Number, fold change, and clonality of TCR clonotypes in HSV lesion site and arm biopsies before and after vaccination. (**a**) Schematic of vaccine study timeline and procedures. CD4+ (**b**) and CD8+ (**c**) T-cell densities from biopsies from control skin at the time of enrollment and from the site of a symptomatic lesion (N=4) are shown in comparison to HSV lesion site and control skin biopsies over the course of a 3-dose vaccine trial in nine vaccine recipients. Each dot represents the mean of three counted sections in a single participant. Median and interquartile range are shown in grey. (**d**) Representative 10x micrographs of CD4+ (green) and CD8+ (red) T-cell density by IFA in HSV lesion site biopsies at specified time points before and after vaccination. CD4+ and CD8+ T-cell IFA from (**e**) control skin and (**f**) lesion site during a symptomatic HSV-2 outbreak. All images are from participant 4. White bars are 100μm. (**g**) Total and (**h**) number of TCRβ clonotypes detected at >4 copies are shown from the HSV lesion site and arm biopsies. (**h**) Clonality calculated from Shannon entropy of the TCR repertoire from each sample. Each dot represents a single participant. Median and interquartile range are shown in grey. For comparisons, *p <0.05, **p <0.01 by paired Wilcoxon.

Fig. 3. Overlap of HSV-2-reactive CD4+ T cells from PBMCs in skin biopsies by clonal tracking. (a) Unique *TRB* sequences detected in blood at day 0 (n=205) and the number of these sequences also detected at day 10 (n=2). (**b**) *TRB* sequences detected in blood at day 10 (n=3285) and the number of these sequences also detected at day 0 (n=5). (**c**) The number of unique TRB nucleotide sequences from HSV-2-reactive CD4+ T cells detected in skin from the arm or the area of HSV-2-reactivation in the same participant at any biopsy time point. (**d**) The proportion of total TRB sequences from the skin that were also detected in PBMCs from day 10 at all time points. For comparisons, *p <0.05 by paired Wilcoxon. (**e**) Overlap by nucleotide sequence between the most prevalent clonotypes sequenced from HSV-2-reactive CD4+ T cells from PBMCs (by IFNg/IL-2 co-expression) in participant 4 and their appearance in the HSV lesion site and arm skin over time, with the corresponding V-J gene identification. T cells from PBMCs in participant 4 on day 10 underwent expansion prior to stimulation and sequencing (**Supplementary Fig. 1**, pathway 2).

Fig. 4. Prevalent and elicited clonotypes in HSV-2-enriched CD4+ T cells from PBMCs ("PBMC"), healed HSV lesion site biopsy ("HSV lesion-area skin"), and arm biopsy expanding or detected at high copy number at dose 1 or 2. (a) Prevalent and (**b**) elicited clonotypes detected in two participants (ID 4 and 6), ranked by fold increase over dose 1 day 0 to day 10.

(**c**) Prevalent or (**d**) elicited clonotypes ranked by fold change over dose 2, selected for those that expanded (from day 0 to day 10 or day 30 to day 40) by >6 fold or were detected at day 10 or day 40 at >6 copies. Each row represents a single clonotype (distinguished by nucleic acid sequence; the corresponding amino acid sequence is shown). The detection of these clones in HSV-2-enriched CD4+ T cells from PBMCs, lesion-area skin and arm skin is compared at each of the tested time points. Number of copies detected in PBMCs from participant 4 at day 10 reflect expansion prior to sequencing and are denoted by $ (see methods). Blank boxes indicate samples where a clonotype was not detected. (**e**) The total number of expanding prevalent (>6-fold change) and highly elicited (>6 copies) clonotypes detected in each participant at day 10. (**f**) The number of prevalent and elicited clonotypes that were detected at day 10 and in 2 or more biopsies after day 10.

Fig. 5. Evaluation of TCRα and β V family and J gene usage. **(a)** shows the shift in oligoclonality of the TCRα sequences in HSV lesion site biopsies on day 0 compared to post-vaccination day 10 in participant 4. X and y axes represent V and J gene families. Z axis "spikes", or the most abundant combinations, are labeled with V and J gene and detected copies. (**b**) CDR3 amino acid sequences and abundance for TCRα (left) and TCRβ (right), shading distinguishes between the established (blue or purple) and novel (red or grey) oligoclonal spikes. (**c**) HSV-2-reactivity of a synthetic TCR comprised of the most abundant TCRα and TCRβ sequences from the day 10 sample in participant 4, using a Jurkat Nur77-mNeonGreen reporter cell system (right). Negative control (no vector, left) and positive control (PMA + Ionomycin, middle) for TCR stimulation and negative treatment (Mock, top) or experimental treatment (UV-irradiated HSV, bottom) to assess TCR specificity.

Fig. 6. Representative data from fine specificity determination of blood CD4 T-cell clones overlapping with TCRβ CDR3 sequences detected in HSV lesion site biopsies. (a) Clonotype tracking with assigned specificity of 15 of the 16 clones queried in participant 4, ranked by abundance and fold change in skin over dose one. Copy numbers in PBMCs are scaled to relative amount of detection owing to different method of sequencing presented for these samples. **(b)** Example of fine-specificity mapping of a single clone confirmed to be specific to UL11. Both specimens were obtained from day 10 after HSV529 vaccination. At left is T-cell proliferation in response to matrix pools of HSV-2 antigens with positive and negative controls. Pools containing US11 (Pool 1, Pool 19) are positive. At right is confirmatory assay with recombinant UL11 and controls. Blue and orange bars represent replicate assays.

Supplementary Table 1. Procedures and study visits
Supplementary Table 2. Demographic characteristics of participants from preliminary work and the vaccine study.

Supplementary Fig. 1. Schema of selection procedures for HSV-2-reactive CD4+ T cells from PBMCs. Pathway 1 represents selection based on intracellular detection of IFN-γ or IL-2 after stimulation with UV-HSV-2. Pathway 2 was performed in PBMCs from participant 4 at day 10 to

validate both methods, after stimulation CD137high CD4+ T cells were expanded, then assayed for cytokine production as above, all cytokine-producing T cells were then submitted for TCRβ sequencing. Flow plots show example of ICS+ sorting in participant 2. Table inset shows the number of cells that were identified to be ICS+ and submitted for sequencing.

Supplementary Fig. 2. Number of PBMC-detected HSV-2-reactive CD4+ TCRβ clonotypes (by comparison of nucleotide sequences) detected in blood at day 0 and at any time point in the skin at the site of HSV-2 reactivation and the arm.

Supplementary Fig. 3. (a) Prevalent and (b) elicited TCRβ clonotypes detected in both HSV-2-reactive CD4+ T cells from PBMCs and skin biopsies ("overlapping clonotypes"), ranked by fold change from day 0 to day 10 in all 9 participants. Each row represents a single TCRβ clonotype (defined by nucleic acid sequence, amino acid listed for readability), number of clonotypes detected are shown for each time point. Comparison is made between PBMCs (left), lesion-area skin (middle) and control skin (right). Blank spots represent a time point where the clonotype was not detected. Participant 1 demonstrated the greatest number of overlapping clonotypes as well as the greatest persistence of these clonotypes over time, but few of these increased in the number of copies from day 0 to day 10. The number of sequences detected in PBMCs at day 10 in participant 4 was increased by the method of detection, where CD137-expressing clonotypes after UV-HSV-2 exposure were expanded prior to selection by ICS and sequencing, these are denoted by $. Two participants (7 and 9) did not have biopsies taken after day 40 and PBMCs from day 0 were not available in participants 6 and 8 (blocks without data are shaded in grey).

Supplementary Fig. 4. Clonal tracking of (a) prevalent and (b) elicited skin-based clonotypes ranked by fold change in abundance of copies from day 0 to day 10 in each participant**.** Clonotypes from all participants were selected for and ranked by fold increase >6 from prior to vaccination to day 10 (prevalent clonotypes) or by increase over single copy to >6 copies at day 10 (elicited clonotypes). Each row represents a single clonotype (defined by nucleic acid sequence, the corresponding amino acid sequence is shown for readability), the number of copies are shown for each time point. Blank spots represent a time point where the clonotype was not detected. Participant 1 had no elicited clonotypes at >6 copies, participant 5 had prevalent clonotypes that expanded at (but not greater than) 6-fold. Two participants (7 and 9) did not have biopsies taken after day 40 and PBMCs from day 0 were not available in participants 6 and 8 (blocks without data are shaded in grey). (**c**) Prevalent and (**d**) elicited clonotypes are ranked by fold increase from day 30 to day 40.

Supplementary Fig. 5. Relative use of Vβ and Jβ genes in TCRβ sequencing from HSV lesion site biopsies by participant and study day in comparison to those seen in HSV-2 reactive CD4+ T cells from PBMCs ("blood") and arm biopsies. Z axis displays numbers of copies in each combination, the height shown is consistent across all time points and sites, insets are shown for PBMC samples. X and y axes represent V and J gene families listed sequentially, not every family is listed for readability. The V and J genes and number of copies is labeled for the most abundant combinations. Copy numbers from arm biopsies are shown as sums from all three

time points: this was less than the peak abundance per biopsy in the HSV lesion site sites with the exception of participant 5. A table of clonotypes of interest is included for participant 8, where a switch in oligoclonal dominance was also seen over dose one (new VJ gene combination at J02-01, V06-06 at day 10, dark blue spike).

Supplementary Fig. 6. HSV-2 UL49-specificity of synthesized TCR from skin-derived TCRα/TCRβ sequencing of a clone observed to establish long-term immunodominance after dose 1 in participant 4. (a) Protein-level specificity in the synthetic TCR from participant 4 and TCR-transduced reporter cell recognition (as measured by expression of mNeonGreen) of HSV-2 UL49 in an antigen concentration-dependent manner in comparison to lack of recognition of UL46. Gating is on live, lymphocyte subset. **(b)** Peptide-level specificity identified by screening of HSV-2 UL49 peptide pools, shown is percentage of cells co-expressing APC+/mNeonGreen+. **(c)** Confirmation of HLA-II use and thus CD4 origination of the TCR by blocking assay using monoclonal antibodies against HLA-DP, DQ, and DR. The TCR-transduced reporter cell line was stimulated with HSV2 strain 186 at final assay dilution of 1:100, 1:1000, or a mock exposure, in the presence of HLA-DP, DR, and DQ blocking antibodies at a final concentration of 1:40, with abrogation of the Nur77-mNeonGreen activation signal in the presence of an HLA-DP monoclonal antibody.

Supplementary Fig. 7. V-J combinations highly suggestive of MAIT cell derivation represent a small minority of the TCRα clonotypes detected in a single individual over time. Prevalence of MAIT-consistent TCRα V-J usage over time in two participants (2 and 4) was approximately 2% of the detected TCRα clones at each time point in both HSV lesion site skin and arm skin biopsies. MAIT-like clones were defined by use of J01-02 in combination with V12, 20, or 33 (**a**). (**b**) shows the relative TCRAJ family usage over time in participants 2 and 4 by percentage of total detected clones at each time point. (**c**) shows the presence of these MAIT-consistent clones in participant 4 over time, defined by nucleic acid sequence and ranked by expansion from day 0 to day 10.

Supplementary Fig. 8. Identification of HSV-2-reactive CD4+ T cells from frozen PBMCs from participant 4 for determination of fine specificity, confirmation of reactivity and bulk sequencing results. (a) Gating scheme for sorting of PBMC from participant 4, day 10 after first dose of HSV529 vaccine. After UV HSV-2 stimulation for 18 hours, brisk up-regulation of surface CD137 was detected and single cells were sorted and clonally expanded. **(b)** Lymphoproliferation results for 192 randomly selected clones presented as a histogram of net CPM for singlicate split-well analyses with whole UV HSV-2 antigen and mock antigen. **(c)** Summary of results of TCR CDR3 sequencing for the 192 CD4+ T-cell clones.

Supplementary methods:

Other inclusion criteria included age 18-55 years, willingness to use contraception for the duration of the study, and willingness to participate. Exclusion criteria included HIV-1 or HCV seropositivity, pregnancy or breast-feeding, BMI >35, serious chronic illness or immunocompromise (including use of immunomodulators).

Fig 1.

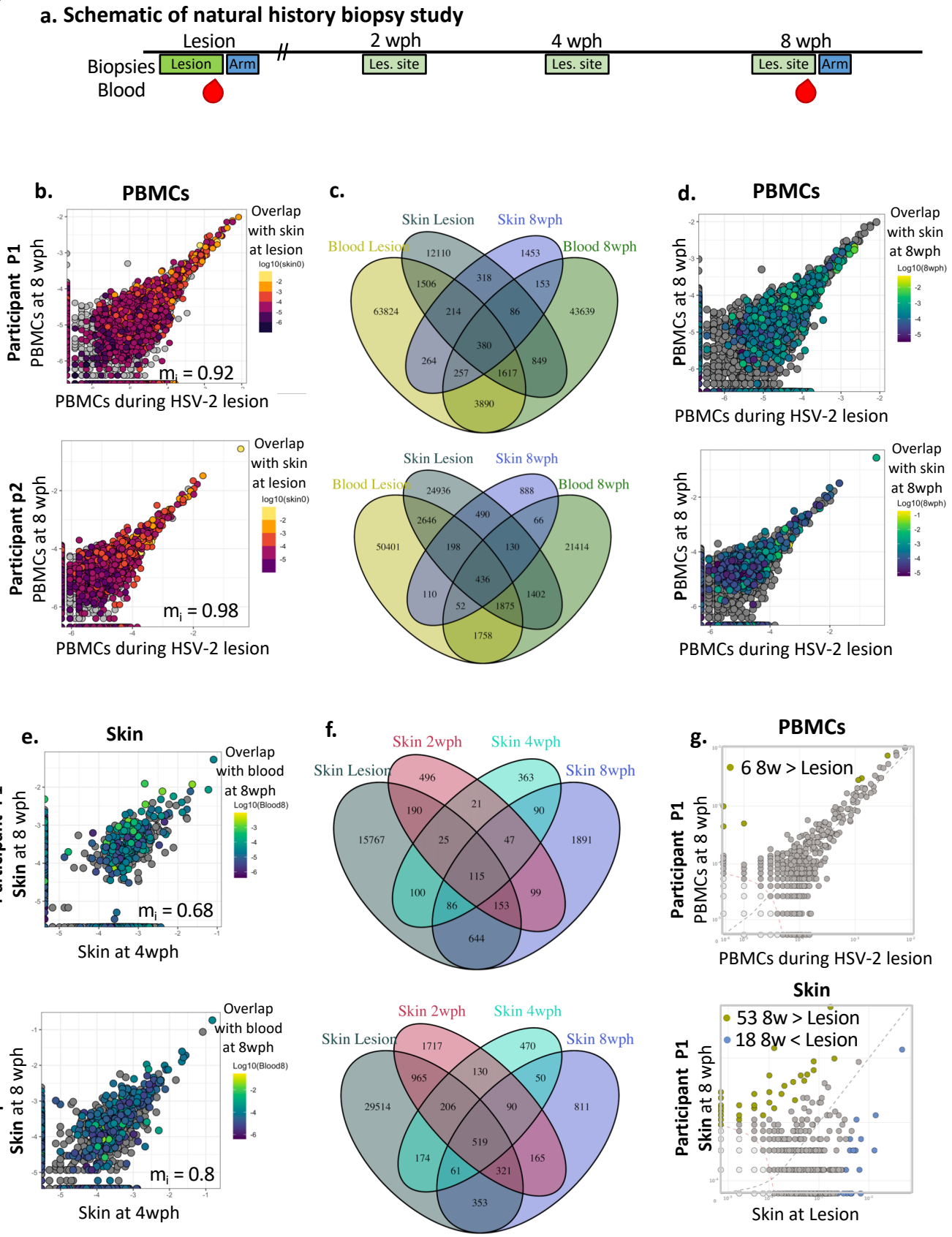
a. Schematic of natural history biopsy study
Lesion
2 wph
4 wph
8 wph
Biopsies
Lesion
Arm
Les. site
Les. site
Les. site
Arm
Blood
b.
PBMCs
Participant P1
PBMCs at 8 wph
Overlap with skin at lesion
log10(skin0)
m_i = 0.92
PBMCs during HSV-2 lesion
Participant p2
PBMCs at 8 wph
Overlap with skin at lesion
log10(skin0)
m_i = 0.98
PBMCs during HSV-2 lesion
c.
Skin Lesion
Skin 8wph
Blood Lesion
Blood 8wph
12110
1453
1506
318
153
63824
214
86
43639
380
264
849
257
1617
3890
Skin Lesion
Skin 8wph
Blood Lesion
Blood 8wph
24936
888
2646
490
66
50401
198
130
21414
436
110
1402
52
1875
1758
d.
PBMCs
PBMCs at 8 wph
Overlap with skin at 8wph
Log10(8wph)
PBMCs during HSV-2 lesion
PBMCs at 8 wph
Overlap with skin at 8wph
Log10(8wph)
PBMCs during HSV-2 lesion
e.
Skin
Participant P1
Skin at 8 wph
Overlap with blood at 8wph
Log10(Blood8)
m_i = 0.68
Skin at 4wph
Participant P2
Skin at 8 wph
Overlap with blood at 8wph
Log10(Blood8)
m_i = 0.8
Skin at 4wph
f.
Skin 2wph
Skin 4wph
Skin Lesion
Skin 8wph
496
363
190
21
90
15767
25
47
1891
115
100
99
86
153
644
Skin 2wph
Skin 4wph
Skin Lesion
Skin 8wph
1717
470
965
130
50
29514
206
90
811
519
174
165
61
321
353
g.
PBMCs
6 8w > Lesion
Participant P1
PBMCs at 8 wph
PBMCs during HSV-2 lesion
Skin
53 8w > Lesion
18 8w < Lesion
Participant P1
Skin at 8 wph
Skin at Lesion

Fig. 2

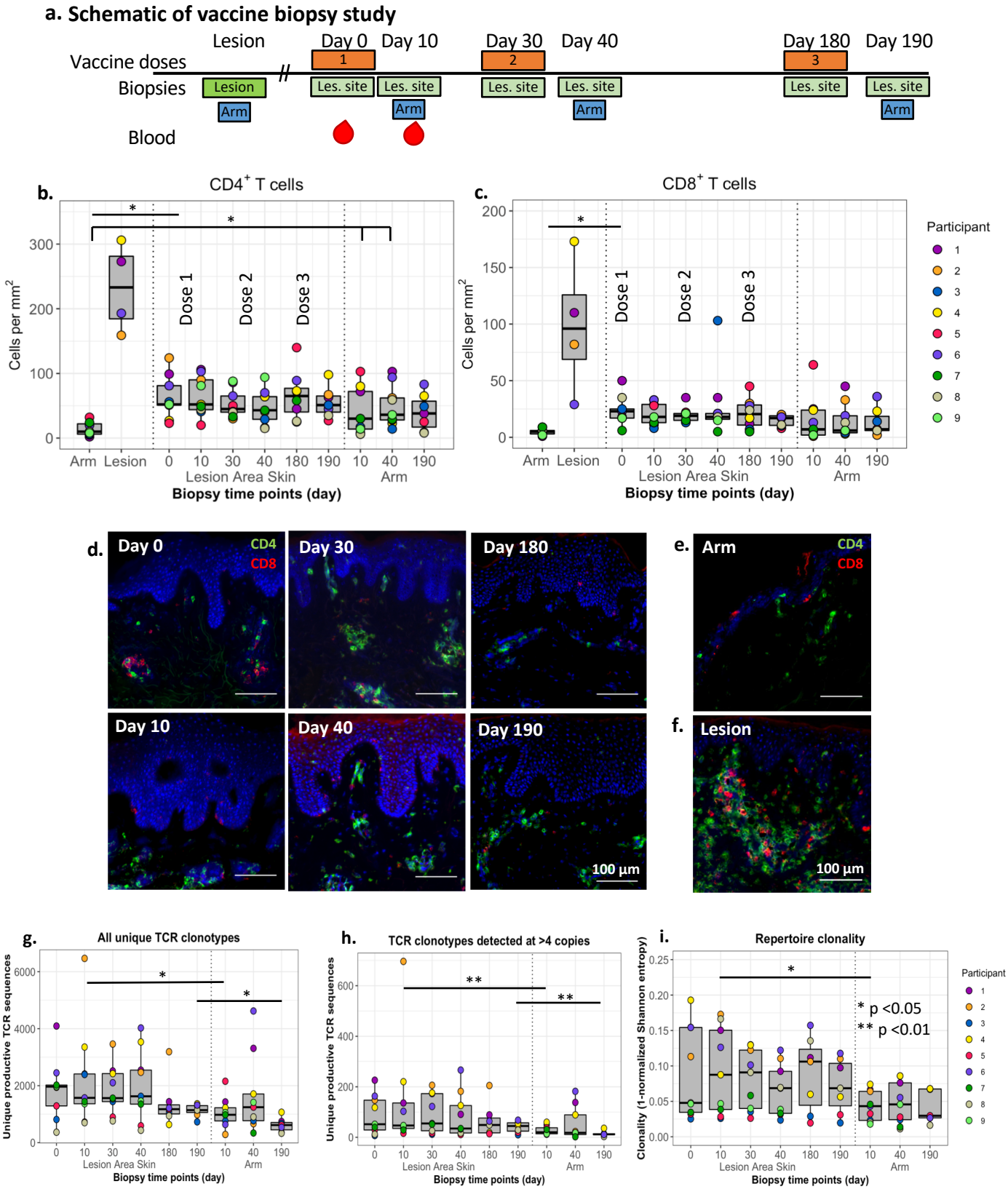
a. Schematic of vaccine biopsy study
Lesion
Day 0
Day 10
Day 30
Day 40
Day 180
Day 190
Vaccine doses
1
2
3
Biopsies
Lesion
Les. site
Arm
Blood
b.
CD4+ T cells
Cells per mm2
Dose 1
Dose 2
Dose 3
Arm
Lesion
Lesion Area Skin
Biopsy time points (day)
c.
CD8+ T cells
Participant
d.
Day 0
Day 30
Day 180
Day 10
Day 40
Day 190
CD4
CD8
100 µm
e.
Arm
f.
Lesion
g.
All unique TCR clonotypes
Unique productive TCR sequences
h.
TCR clonotypes detected at >4 copies
i.
Repertoire clonality
Clonality (1-normalized Shannon entropy)
* p <0.05
** p <0.01

Fig. 3

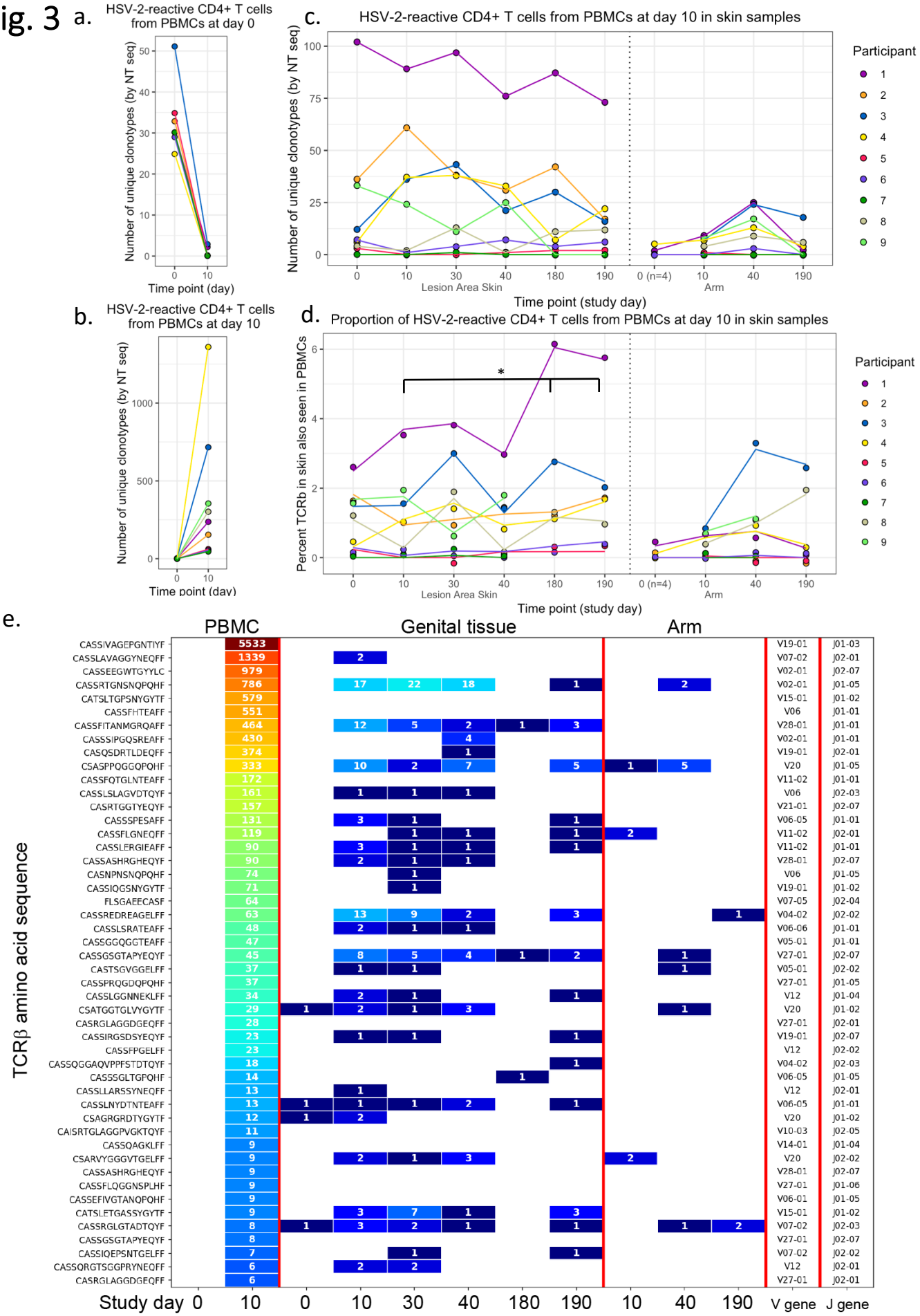
a.
HSV-2-reactive CD4+ T cells from PBMCs at day 0
Number of unique clonotypes (by NT seq)
Time point (day)
b.
HSV-2-reactive CD4+ T cells from PBMCs at day 10
Number of unique clonotypes (by NT seq)
Time point (day)
c.
HSV-2-reactive CD4+ T cells from PBMCs at day 10 in skin samples
Number of unique clonotypes (by NT seq)
Lesion Area Skin
Arm
Time point (study day)
Participant
d.
Proportion of HSV-2-reactive CD4+ T cells from PBMCs at day 10 in skin samples
Percent TCRb in skin also seen in PBMCs
Lesion Area Skin
Arm
Time point (study day)
Participant
e.
PBMC
Genital tissue
Arm
TCRβ amino acid sequence
Study day
V gene
J gene

Fig. 4

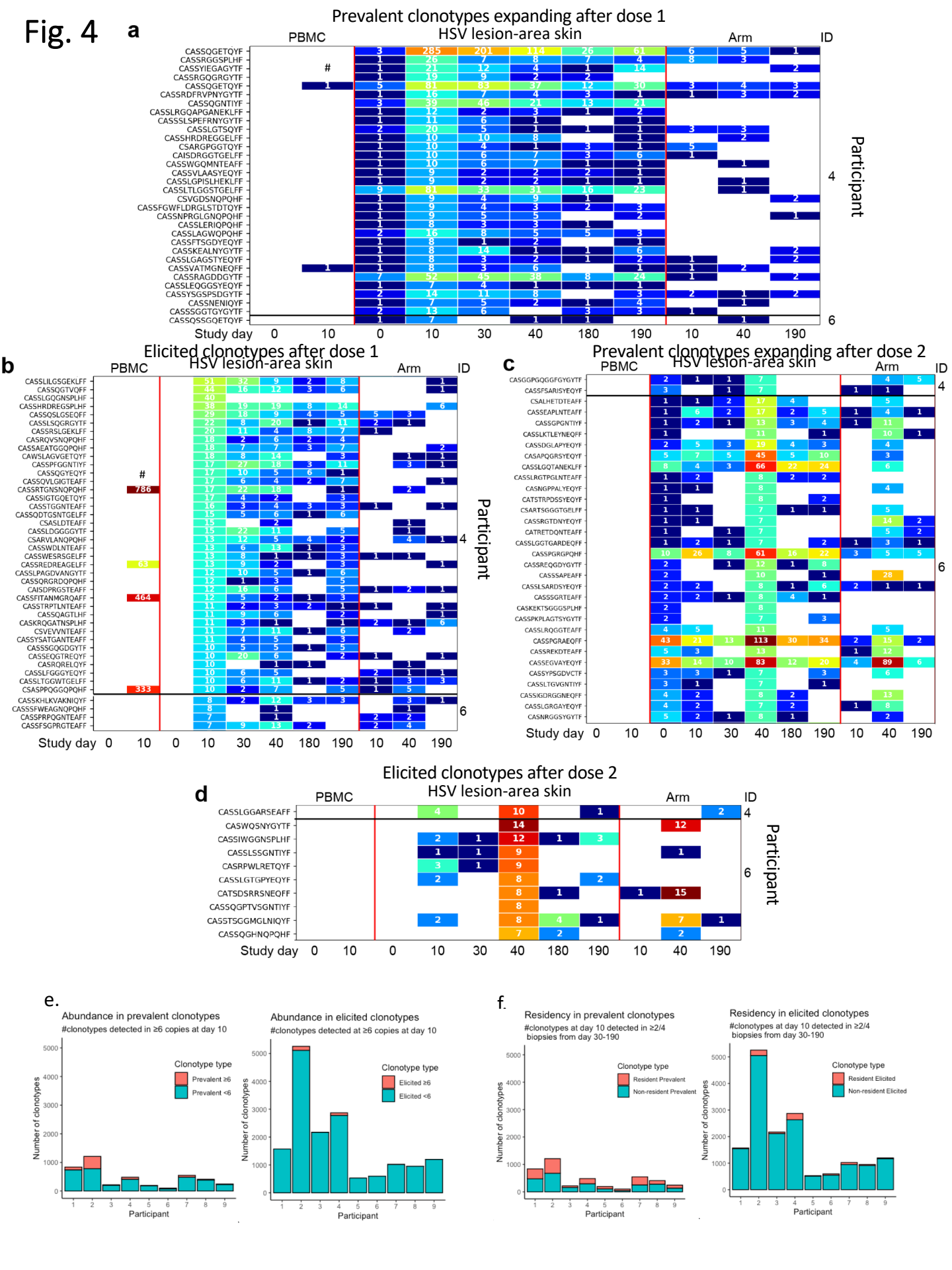
a
Prevalent clonotypes expanding after dose 1
PBMC
HSV lesion-area skin
Arm
ID
Participant
Study day
b
Elicited clonotypes after dose 1
c
Prevalent clonotypes expanding after dose 2
d
Elicited clonotypes after dose 2
e.
Abundance in prevalent clonotypes
#clonotypes detected in ≥6 copies at day 10
Clonotype type
Prevalent ≥6
Prevalent <6
Abundance in elicited clonotypes
#clonotypes detected at ≥6 copies at day 10
Elicited ≥6
Elicited <6
Number of clonotypes
Participant
f.
Residency in prevalent clonotypes
#clonotypes at day 10 detected in ≥2/4 biopsies from day 30-190
Resident Prevalent
Non-resident Prevalent
Residency in elicited clonotypes
#clonotypes at day 10 detected in ≥2/4 biopsies from day 30-190
Resident Elicited
Non-resident Elicited

Figure 5.

a.

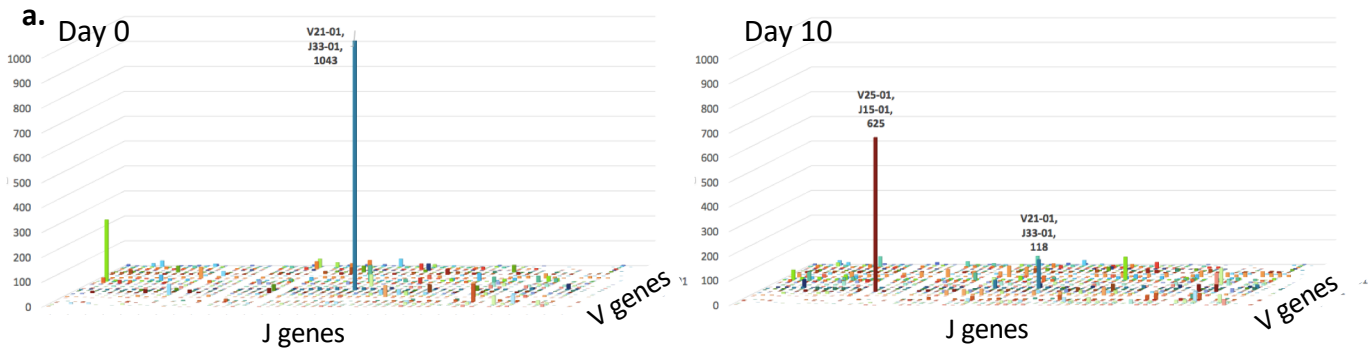
Day 0
V21-01, J33-01, 1043
J genes
V genes
Day 10
V25-01, J15-01, 625
V21-01, J33-01, 118
J genes
V genes

b.

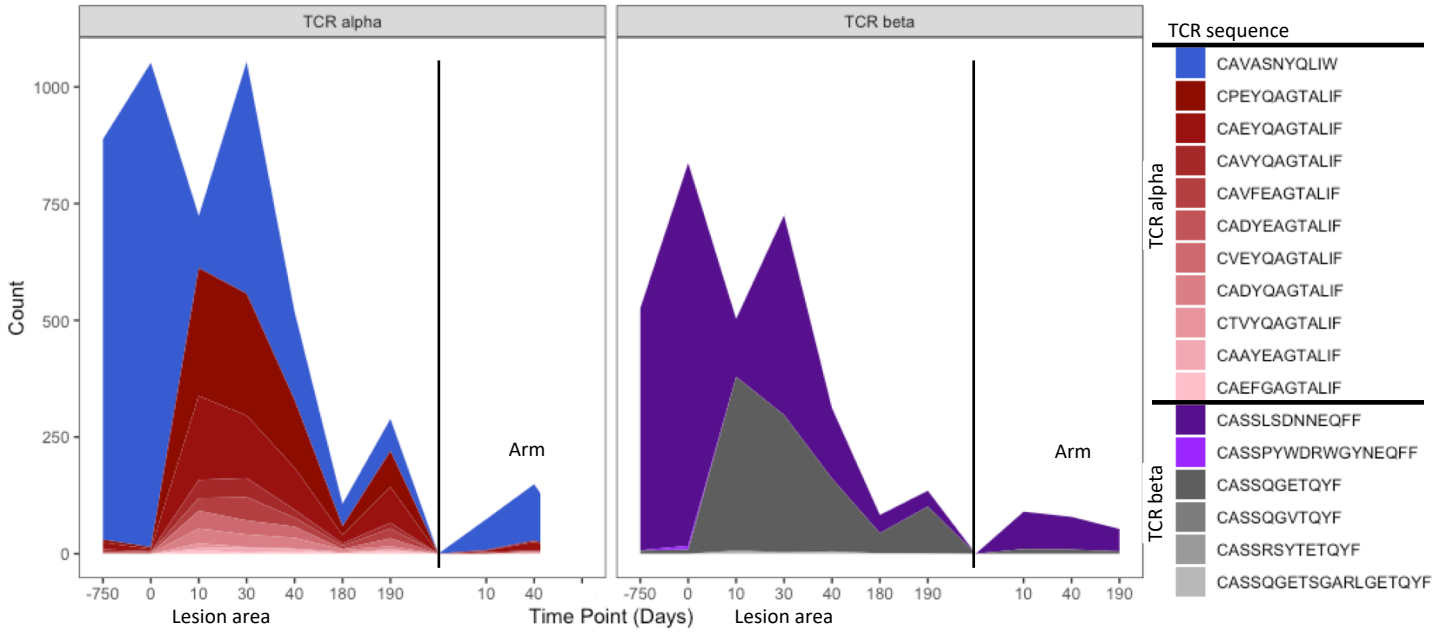
TCR alpha
TCR beta
Count
Arm
Lesion area
Time Point (Days)
TCR sequence
TCR alpha
CAVASNYQLIW
CPEYQAGTALIF
CAEYQAGTALIF
CAVYQAGTALIF
CAVFEAGTALIF
CADYEAGTALIF
CVEYQAGTALIF
CADYQAGTALIF
CTVYQAGTALIF
CAAYEAGTALIF
CAEFGAGTALIF
TCR beta
CASSLSDNNEQFF
CASSPYWDRWGYNEQFF
CASSQGETQYF
CASSQGVTQYF
CASSRSYTETQYF
CASSQGETSGARLGETQYF

c.

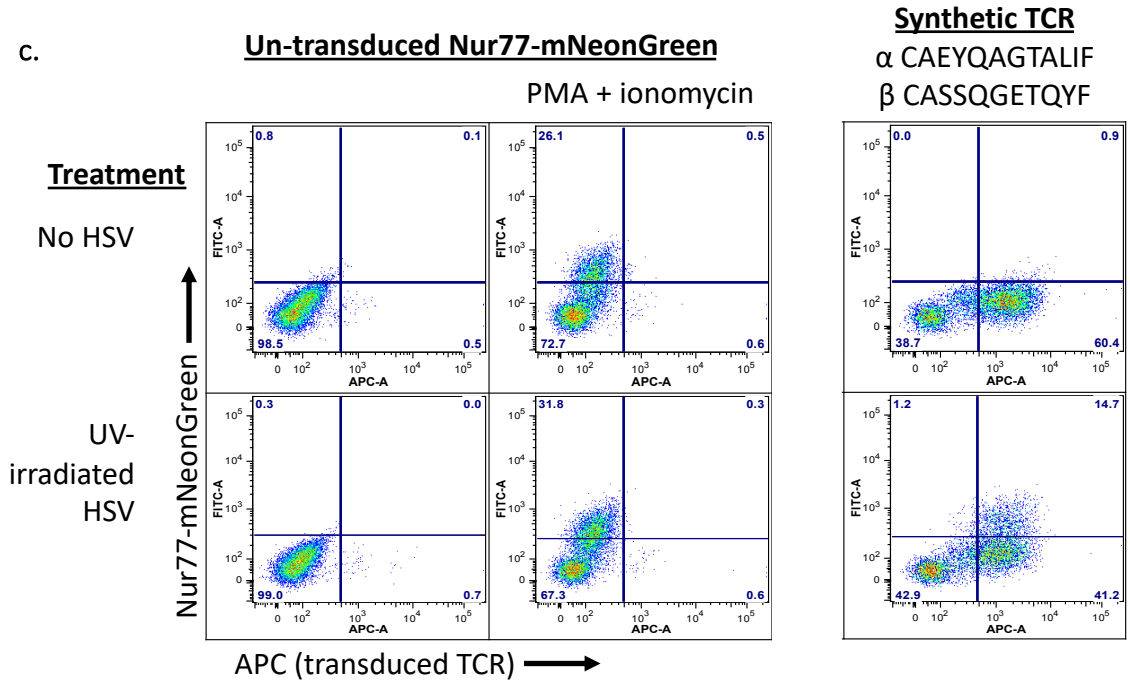
Un-transduced Nur77-mNeonGreen
PMA + ionomycin
Synthetic TCR
α CAEYQAGTALIF
β CASSQGETQYF
Treatment
No HSV
UV-irradiated HSV
Nur77-mNeonGreen
APC (transduced TCR)
FITC-A
APC-A
0.8
0.1
98.5
0.5
26.1
0.5
72.7
0.6
0.0
0.9
38.7
60.4
0.3
0.0
99.0
0.7
31.8
0.3
67.3
0.6
1.2
14.7
42.9
41.2

Figure 6.

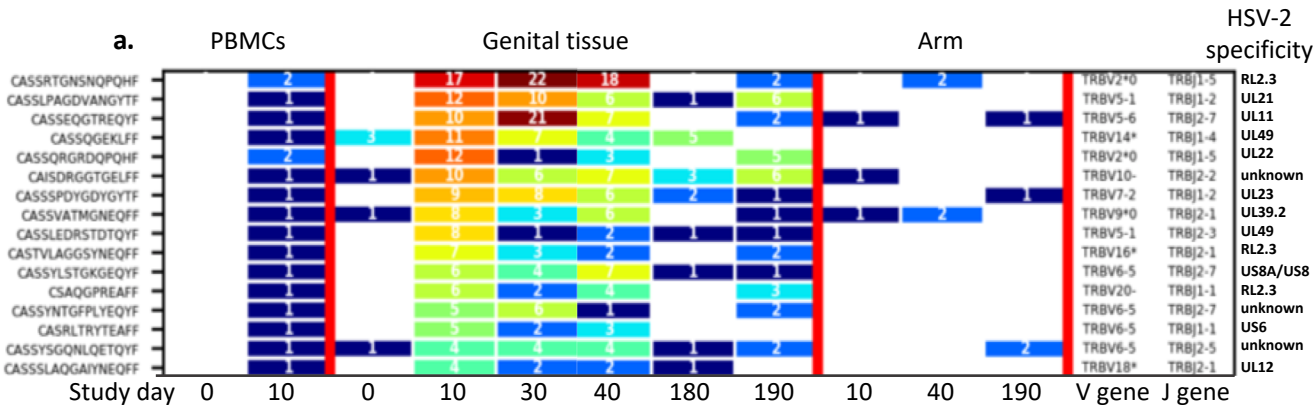
a.
PBMCs
Genital tissue
Arm
HSV-2 specificity
CASSRTGNSNQPQHF
CASSLPAGDVANGYTF
CASSEQGTREQYF
CASSQGEKLFF
CASSQRGRDQPQHF
CAISDRGGTGELFF
CASSSPDYGDYGYTF
CASSVATMGNEQFF
CASSLEDRSTDTQYF
CASTVLAGGSYNEQFF
CASSYLSTGKGEQYF
CSAQGPREAFF
CASSYNTGFPLYEQYF
CASRLTRYTEAFF
CASSYSGQNLQETQYF
CASSSLAQGAIYNEQFF
TRBV2*0 TRBJ1-5 RL2.3
TRBV5-1 TRBJ1-2 UL21
TRBV5-6 TRBJ2-7 UL11
TRBV14* TRBJ1-4 UL49
TRBV2*0 TRBJ1-5 UL22
TRBV10- TRBJ2-2 unknown
TRBV7-2 TRBJ1-2 UL23
TRBV9*0 TRBJ2-1 UL39.2
TRBV5-1 TRBJ2-3 UL49
TRBV16* TRBJ2-1 RL2.3
TRBV6-5 TRBJ2-7 US8A/US8
TRBV20- TRBJ1-1 RL2.3
TRBV6-5 TRBJ2-7 unknown
TRBV6-5 TRBJ1-1 US6
TRBV6-5 TRBJ2-5 unknown
TRBV18* TRBJ2-1 UL12
Study day 0 10 0 10 30 40 180 190 10 40 190 V gene J gene

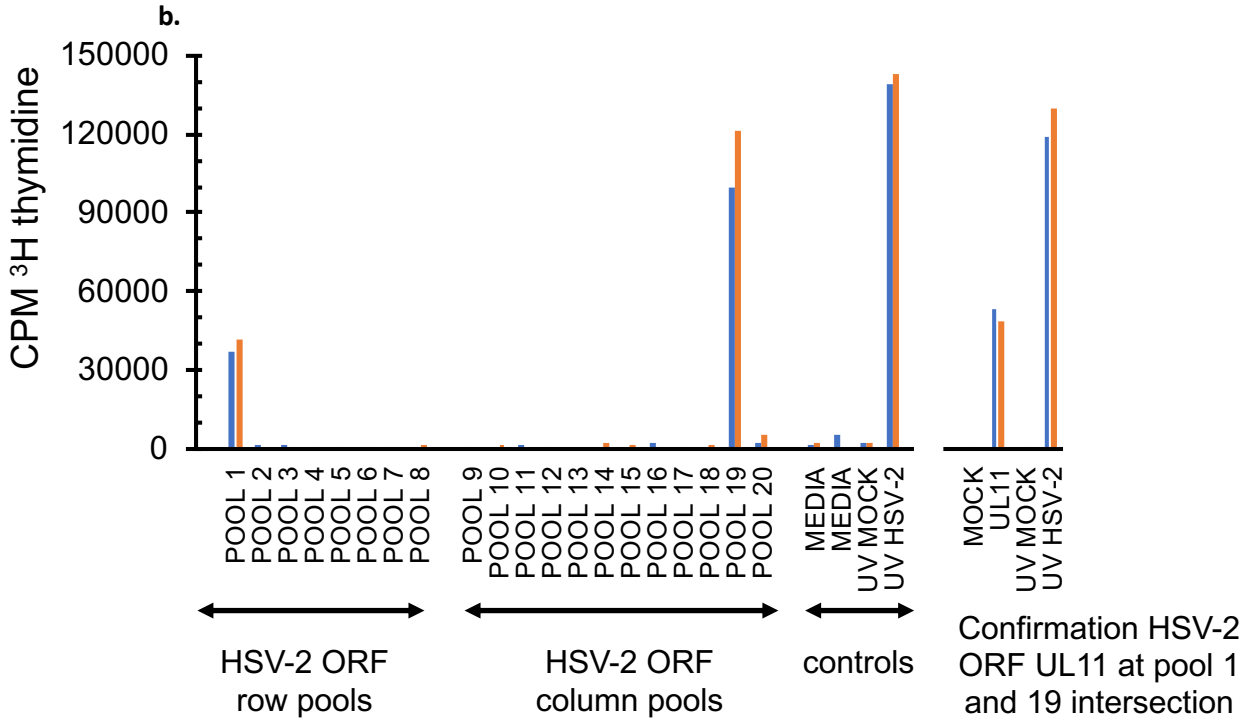
b.
CPM ³H thymidine
150000
120000
90000
60000
30000
0
POOL 1
POOL 2
POOL 3
POOL 4
POOL 5
POOL 6
POOL 7
POOL 8
POOL 9
POOL 10
POOL 11
POOL 12
POOL 13
POOL 14
POOL 15
POOL 16
POOL 17
POOL 18
POOL 19
POOL 20
MEDIA
MEDIA
UV MOCK
UV HSV-2
MOCK
UL11
UV MOCK
UV HSV-2
HSV-2 ORF row pools
HSV-2 ORF column pools
controls
Confirmation HSV-2 ORF UL11 at pool 1 and 19 intersection